10/11/1995 JSO (1)

LBL-35976
UC-800

Lawrence Berkeley Laboratory
UNIVERSITY OF CALIFORNIA

EARTH SCIENCES DIVISION

Hydraulic Conductivity of Rock Fractures

R.W. Zimmerman and G.S. Bodvarsson

October 1994

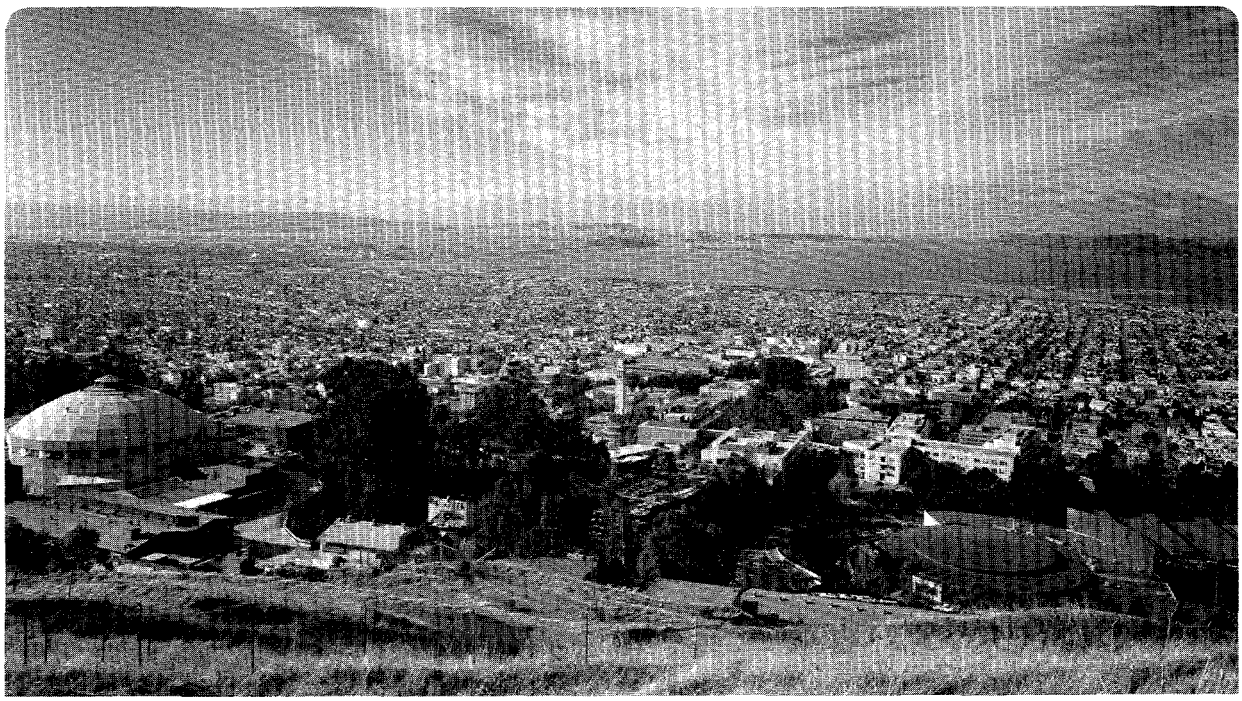

Prepared for the U.S. Department of Energy under Contract Number DE-AC03-76SF00098

DISTRIBUTION OF THIS DOCUMENT IS UNLIMITED

DISCLAIMER

This document was prepared as an account of work sponsored by the United States Government. Neither the United States Government nor any agency thereof, nor The Regents of the University of California, nor any of their employees, makes any warranty, express or implied, or assumes any legal liability or responsibility for the accuracy, completeness, or usefulness of any information, apparatus, product, or process disclosed, or represents that its use would not infringe privately owned rights. Reference herein to any specific commercial product, process, or service by its trade name, trademark, manufacturer, or otherwise, does not necessarily constitute or imply its endorsement, recommendation, or favoring by the United States Government or any agency thereof, or The Regents of the University of California. The views and opinions of authors expressed herein do not necessarily state or reflect those of the United States Government or any agency thereof or The Regents of the University of California and shall not be used for advertising or product endorsement purposes.

Lawrence Berkeley Laboratory is an equal opportunity employer.

DISCLAIMER

Portions of this document may be illegible in electronic image products. Images are produced from the best available original document.

LBL-35976
UC-800

Hydraulic Conductivity of Rock Fractures

Robert W. Zimmerman and Gudmundur S. Bodvarsson

Earth Sciences Division
Lawrence Berkeley Laboratory
University of California
Berkeley, CA 94720

October 1994

This work was carried out under Department of Energy Contract No. DE-AC03-76SF00098 for the Director, Office of Civilian Radioactive Waste Management, Office of Geologic Disposal, and was administered by the Nevada Operations Office, U. S. Department of Energy, in cooperation with the U. S. Geological Survey, Denver.

MASTER

DISTRIBUTION OF THIS DOCUMENT IS UNLIMITED

Hydraulic Conductivity of Rock Fractures

Robert W. Zimmerman and Gudmundur S. Bodvarsson

Earth Sciences Division
Lawrence Berkeley Laboratory
University of California
Berkeley, CA 94720

ABSTRACT

The problem of the flow of a single-phase fluid through a rough-walled rock fracture is discussed within the context of rigorous fluid mechanics. The derivation of the "cubic law" is given as the solution to the Navier-Stokes equations for flow between smooth, parallel plates, the only fracture geometry that is amenable to exact treatment. The various geometric and kinematic conditions that are necessary in order for the Navier-Stokes equations to be replaced by the more tractable lubrication or Hele-Shaw equations are studied and quantified. In general, this requires a sufficiently low flow rate, and some restrictions on the spatial rate of change of the aperture profile. Various analytical and numerical results are reviewed pertaining to the problem of relating the effective hydraulic aperture to the statistics of the aperture distribution. These studies all lead to the conclusion that the effective hydraulic aperture is always less than the mean aperture, by a factor that depends on the ratio of the mean value of the aperture to its standard deviation. The tortuosity effect caused by regions where the rock walls are in contact with each other is studied using the Hele-Shaw equations, leading to a simple correction factor that depends on the area fraction occupied by the contact regions. Finally, the predicted hydraulic apertures are compared to measured values for eight data sets from the literature for which aperture and conductivity data were available on the same fracture. It is found that reasonably accurate predictions of hydraulic conductivity can be made based solely on the first two moments of the aperture distribution function, and the proportion of contact area.

Table of Contents

Introduction

In many geological formations with low matrix permeability, fluid flow takes place predominantly through fractures. In some cases the bulk of the flow takes place through a single fracture or fault, while in other cases the flow occurs through a network of fractures. In either case, an understanding is needed of how fluid flows through a single rough-walled rock fracture. Fracture-dominated flow is important in many situations of technical or scientific interest, such as in certain naturally-fractured petroleum reservoirs, for many geothermal reservoirs, and in many underground waste isolation problems. Yucca Mountain, Nevada, for example, which is a potential site of a U. S. Department of Energy underground radioactive waste repository, contains numerous geological units that are highly fractured. A clear understanding of the hydraulic conductivity of fractures has therefore been identified as an important scientific problem that must be addressed during the site characterization process at Yucca Mountain (Gomberg, 1991).

In this report, we address the question of how to relate the hydraulic conductivity of a fracture to the geometry and topography of the fracture walls and asperities. We do this by starting with the Navier-Stokes equations, which govern the flow of a single-phase fluid, systematically simplify the equations to reduce them to manageable form, while carefully considering the conditions required for the various approximations to be valid. We then discuss and review various analytical and numerical studies that have been done for different types of fracture geometry models. The aim of this discussion is to arrive at an equation that will relate the fracture conductivity to a small number of basic geometrical parameters, such as the mean aperture, fractional contact area, etc. Finally, we compare the various theoretical models to a few sets of data that have been found in the literature in which conductivities and aperture statistics have been measured on the same rock fractures.

There are other fracture properties that are not directly addressed in this report, such as those that control two-phase flow and solute transport. However, a clear understanding of single-phase flow in a rough-walled rock fracture is a prerequisite to the development of both two-phase flow models and solute transport models. Most models of two-phase flow in fractures (i.e., Pruess and Tsang, 1990; Murphy and Thomson, 1993) assume that each phase follows a local version of the cubic law, which rigorously applies only to single-phase flow in a smooth-walled fracture. Hence, an understanding of the limitations, if any, of the cubic law for single-phase flow is certainly needed for the further refinement of two-phase flow models. Solute transport models also often utilize the velocity profile that occurs during flow through a smooth-walled fracture (i.e., Horne and Rodriguez, 1983). Any deviation from this profile caused by wall roughness or asperity contact will have an effect on solute transport. In fact, the tortuous streamlines that the fluid follows as it flows around the asperities constitute a primary mechanism for lateral dispersion.

Basic Equations Governing Fluid Flow

The flow of an incompressible Newtonian viscous fluid is governed by the following form of the Navier-Stokes equations (Batchelor, 1967, pp. 147-150):

$$\frac{\partial \mathbf{u}}{\partial t} + (\mathbf{u}\cdot\nabla)\mathbf{u} = \mathbf{F} - \frac{1}{\rho}\nabla p + \frac{\mu}{\rho}\nabla^2\mathbf{u}, \qquad (1)$$

where ρ is the fluid density, $\mathbf{F}$ is the body force vector (per unit mass), p is pressure, μ is the fluid viscosity, and $\mathbf{u}$ is the velocity vector. The first term on the left represents the acceleration of a fluid particle due to the fact that, at a fixed point in space, the velocity may vary with time. The second term is the advective acceleration term, which accounts for the fact that, even in steady-state flow, a given fluid particle

may change its velocity (i.e., be accelerated) by virtue of moving to a position at which there is a different velocity. The sum of these two terms represents the acceleration of a fluid particle computed by "following the particle" along its trajectory. The term $(\mathbf{u}\cdot\nabla)\mathbf{u}$ can be interpreted as the scalar operator $\mathbf{u}\cdot\nabla$ operating on the vector $\mathbf{u}$. The forcing terms on the right-hand side represent the applied body force, the applied pressure gradient, and the viscous forces.

Eq. (1) represents one vector equation, or three scalar equations, containing four functions: three velocity components and the pressure field. In order to have a closed system of equations, they must be supplemented by the so-called continuity equation, which represents conservation of mass. For an incompressible fluid, conservation of mass is equivalent to conservation of volume, and the equation takes the form

$$div\,\mathbf{u} \equiv \nabla\cdot\mathbf{u} = 0\,. \tag{2}$$

The assumption of incompressibility is acceptable for liquids under typical subsurface conditions. For example, as the compressibility of water is only 4.9×10^{-10}/Pa (Batchelor, 1967, p. 595), a pressure change of 1 MPa (10 bars) changes the density by only 0.05%. This compressibility effect is important for transient problems, since it contributes to the storativity of the rock/fluid system. However, since the relationship between permeability and fracture geometry is most readily studied using steady-state processes, transient effects can be ignored for the present purposes, and the fluid density can be assumed to be constant. The relevant boundary conditions for the Navier-Stokes equations include the so-called "no-slip" conditions, which specify that at any boundary between the fluid and a solid, the velocity vector of the fluid must equal that of the solid (Batchelor, 1967, p. 149). This implies that at the fracture walls, not only is the normal component of the velocity equal to zero, but the tangential component vanishes as well.

The most common situation in subsurface flow is for the only appreciable body force to be that due to gravity, in which case $\mathbf{F}=\mathbf{g}$. Taking the z direction to be vertically upwards, we have $\mathbf{g}=-g\,\mathbf{e_z}$, where $g = 9.81\,\mathrm{m/s^2} = 9.81\,\mathrm{N/kg}$, and $\mathbf{e}_z$ is a unit vector in the vertical direction. The gravitational term can be removed from the governing equations by defining a reduced pressure (Batchelor, 1967 p. 176; Phillips, 1991, p. 26) as

$$\hat{p} = p + \rho g z \,, \tag{3}$$

in which case the two terms $\mathbf{F} - (1/\rho)\nabla p$ can be written as

$$\mathbf{F} - \frac{1}{\rho}\nabla p = -g\,\mathbf{e}_z - \frac{1}{\rho}\nabla p = \frac{-1}{\rho}(\nabla p + \rho g\,\mathbf{e}_z) = \frac{-1}{\rho}\nabla(p + \rho g z) = \frac{-1}{\rho}\nabla\hat{p} \,. \tag{4}$$

Hence, the governing equations can be written without the gravitational term, as long as it is understood that the pressure represents the reduced pressure, as defined in eq. (3), and the density is assumed constant. For simplicity of notation, we will use p, with the understanding that it actually represents the reduced pressure $\hat{p}$.

Fracture permeability is generally defined under the assumption of steady-state flow under a uniform macroscopic pressure gradient. In the steady-state, the term $\partial\mathbf{u}/\partial t$ drops out, and the equations reduce to

$$\mu\nabla^2\mathbf{u} - \rho(\mathbf{u}\cdot\nabla)\mathbf{u} = \nabla p \,. \tag{5}$$

The presence of the advective component of the acceleration, $(\mathbf{u}\cdot\nabla)\mathbf{u}$, generally causes the equations to be nonlinear, and consequently very difficult to solve. In certain cases

this term is either very small, in which case it can be neglected, or else vanishes altogether. The case of steady flow between parallel plates is one in which the advective terms vanish identically, thus allowing an exact solution to be obtained, as will be shown below. If any other more realistic geometry is to be considered as a model of a rock fracture, approximations must be made to linearize the Navier-Stokes equations, or otherwise reduce them to tractable form. Some of these resulting approximate equations, such as the Reynolds and Hele-Shaw equations, are discussed below.

Parallel Plate Model and Cubic Law

The simplest model of flow through a rock fracture is the so-called parallel plate model, in which the fracture is assumed to be bounded by two smooth, parallel walls separated by an aperture h. This is actually the only geometrical fracture model for which an exact calculation of the hydraulic conductivity is possible; this calculation yields the well-known "cubic law" (Witherspoon et al., 1980). Despite its assumption of an overly-simplified fracture geometry, this model is still widely-used in subsurface flow modeling. Furthermore, most other models can be considered to be refinements of the parallel plate model to include the effects of wall roughness, asperity contacts, etc. It is therefore worthwhile to study the parallel plate model in detail.

Assume that the fracture walls can be represented by two smooth, parallel plates that are separated by an aperture h, as in Fig. 1. Now imagine that there is a uniform pressure gradient within the plane of the fracture. This can be accomplished, for example, by holding two opposing edges of the fracture at pressures p_i and p_o, respectively (see Fig. 1a), in which case the magnitude of the macroscopic pressure gradient is $(p_i - p_o)/L$. This magnitude will also be denoted by $|\overline{\nabla p}|$, where the overbar denotes an average over the plane of the fracture. We now set up a Cartesian coordinate system which has its $x_1 \equiv x$ direction parallel to ∇p, its $x_2 \equiv y$ direction lying perpendicular to x_1 in the plane of the fracture, and its direction $x_3 \equiv z$ perpendicular to

the fracture walls. The top and bottom walls of the fracture correspond to $z = \pm h/2$. Note that this z direction is not necessarily vertical.

The (reduced) pressure gradient lies entirely in the plane of the fracture, and has no z component. It seems plausible that the velocity will also have no z component, particularly since u_z must not only vanish at the two walls of the fracture, $z = \pm h/2$, but must also have a mean value of zero. Since the geometry of the region between the plates does not vary with x or y, the pressure gradient should also be uniform within the plane of the fracture. Hence we assume that the velocity vector depends only on z. Note that as all components of the velocity must vanish at $z = \pm h/2$, the velocity vector must necessarily vary with z. The components of the vector $(\mathbf{u}\cdot\nabla)\mathbf{u}$ can be written explicitly as

$$(\mathbf{u}\cdot\nabla)\mathbf{u} = (\mathbf{u}\cdot\nabla)(u_x, u_y, u_z) = \left[\mathbf{u}\cdot(\nabla u_x),\ \mathbf{u}\cdot(\nabla u_y),\ \mathbf{u}\cdot(\nabla u_z)\right]. \tag{6}$$

As the velocity components do not vary with x or y, any of the three velocity gradients that are not identically zero must be present in the z direction, whereas the velocity vector resides in the $x-y$ plane. Hence, each of the dot products in eq. (6) is zero. This serves to remove the nonlinear term from eq. (5), leaving

$$\mu\nabla^2\mathbf{u}(z) = \nabla p\ . \tag{7}$$

Now recall that ∇p lies parallel to the x axis, and can be written as

$$\nabla p = \left[\frac{\partial p}{\partial x}, \frac{\partial p}{\partial y}, \frac{\partial p}{\partial z}\right] = \left[|\overline{\nabla p}|, 0, 0\right]. \tag{8}$$

Comparison of eqs. (7) and (8) show that the three velocity components must satisfy the following three equations:

$$\nabla^2 u_x(z) = \frac{|\overline{\nabla p}|}{\mu}, \qquad \nabla^2 u_y(z) = 0, \qquad \nabla^2 u_z(z) = 0. \tag{9}$$

The boundary conditions for each velocity component are that $u_i = 0$ when $z = \pm h/2$. It is obvious that $u = 0$ will satisfy the governing equations for u_y and u_z, and their associated boundary conditions. To find u_x, we integrate eq. (9a) twice with respect to z, and make use of the boundary conditions, yielding

$$u_x(z) = \frac{|\overline{\nabla p}|}{2\mu}\left[z^2 - (h/2)^2\right]. \tag{10}$$

Finally, we must verify that this velocity satisfies the continuity equation (2):

$$\nabla \cdot \mathbf{u} = \frac{\partial u_x}{\partial x} + \frac{\partial u_y}{\partial y} + \frac{\partial u_z}{\partial z} = 0, \tag{11}$$

since $u_y = u_z = 0$, and u_x depends only on z, but not on x.

The velocity profile given by eq. (10) is parabolic, and symmetric about the midplane of the fracture (see Fig. 1b). The velocity vanishes at the fracture walls, and is largest along the midplane, where its magnitude is $|\overline{\nabla p}|h^2/8\mu$. The total volumetric flux through the fracture, for a width w in the y direction (perpendicular to the pressure gradient), is found by integrating the velocity across the fracture from $z = -h/2$ to $z = +h/2$:

$$Q = w \int_{-h/2}^{+h/2} u_x(z)\,dz = w \int_{-h/2}^{+h/2} \frac{|\overline{\nabla p}|}{2\mu}[z^2 - (h/2)^2]dz = \frac{-|\overline{\nabla p}|wh^3}{12\mu}. \qquad (12)$$

The minus sign indicates that the flux is in the direction opposite to the pressure gradient, which is to say the fluid flows from regions of high pressure to regions of low pressure. The average velocity can be found by dividing the flux by the cross-sectional area, wh:

$$\bar{u}_x = \frac{-|\overline{\nabla p}|h^2}{12\mu}. \qquad (13)$$

Now recall Darcy's law for flow through porous media, which in one dimension can be written as (de Marsily, 1986, p. 56)

$$Q = \frac{-kA|\overline{\nabla p}|}{\mu}. \qquad (14)$$

Since the cross-sectional area A is equal to wh, comparison of eqs. (12) and (14) shows that the permeability of the fracture can be identified as

$$k = \frac{h^2}{12}. \qquad (15)$$

The product of the permeability and area, kA, which is sometimes known as the transmissivity, is equal to

$$T \equiv kA = \frac{wh^3}{12}, \qquad (16)$$

which expresses the so-called cubic law. An important consequence of the cubic law is that the fracture transmissivity is extremely sensitive to the size of the aperture.

Although the transmissivity calculated for the parallel plate model, given by eq. (16), is often referred to as the cubic law, the dependence of T on h^3 is actually a consequence of the fact that the equations must be dimensionally consistent. Since Q has dimensions of [m^3/s], the pressure drop has dimensions of [Pa], the length L has dimensions of [L], and μ has dimensions of [Pa·s], T must have dimensions of [m^4]. As it is obvious that the total flux must scale linearly with the depth w perpendicular to the direction of flow, T must therefore scale with the cube of the aperture. Hence, the transmissivity can necessarily be written as $T = Cwh^3$, where C is a dimensionless parameter. From this point of view, it may be said that the main prediction of the parallel plate model is that $C = 1/12$.

Deviations from the Cubic Law

The cubic law was derived under the assumption that the fracture could be modeled as the region bounded by two smooth, parallel plates. For this geometry, it is an exact result. Real rock fractures, however, have rough walls, and, hence, have variable apertures. Furthermore, there are usually regions where the two opposing faces of the fracture wall are in contact with each other, effectively reducing the aperture to zero. Since transmissivity is proportional to h^3, fluid flowing in a variable-aperture fracture under saturated conditions will tend to follow paths of least resistance, which is to say paths of largest aperture. This will cause the fluid particles to depart from the rectilinear streamlines found for the parallel plate model. Contact regions between the opposing fracture walls will cause the streamlines to follow tortuous paths, as the fluid particles flow around the obstructions. Each of these factors has the effect of invalidating the conditions under which the cubic law was derived.

In order to apply the cubic law to the prediction of the transmissivity of a real rock fracture, one could assume that eq. (16) still holds if the aperture h is replaced by the mean aperture $<h>$. This is sometimes taken to be an alternate definition of the cubic law, i.e., (cf., Brown, 1987)

$$T = \frac{w<h>^3}{12}. \tag{17}$$

Although eq. (17) is in some sense a first approximation to the actual transmissivity of a rough or obstructed fracture, the effects of roughness and obstructions are not properly accounted for by merely replacing h with $<h>$, as will be shown in detail below. This suggests that we define the so-called hydraulic aperture h_H to be that value that allows the transmissivity to be defined by the ''cubic-law'', i.e.,

$$T = \frac{wh_H^3}{12}. \tag{18}$$

Hence, the problem of relating the transmissivity of a fracture to its geometry can be thought of in terms of finding an expression for the hydraulic aperture h_H. This requires solution of the Navier-Stokes equations in fracture geometries that include varying aperture and obstructed regions. These solutions have only be obtained by approximate means, in which the Navier-Stokes equations are first reduced to simpler governing equation(s).

Another possible cause of deviations from the cubic law is turbulence. Although the velocity profile found above for the parallel plate model was derived using various plausible assumptions and educated guesses, it can be rigorously verified by substitution back into the Navier-Stokes equations, and then also checking that the boundary

conditions are satisfied; the continuity equation was verified in eq. (11). This raises, however, the question of whether or not this solution is the *unique* solution to the problem of flow between two smooth parallel plates under a uniform pressure gradient. In general, there is no uniqueness theorem for the full Navier-Stokes equations, as there is, say, in the theory of linear elasticity (Sokolnikoff, 1956, pp. 86-89). In fact, at sufficiently high velocities, the laminar velocity profile derived above, although still a legitimate solution to the governing equations, will become unstable, giving way to turbulent flow (e.g., Sherman, 1990, Chapter 13). This transition will typically occur when the Reynolds number, defined here by

$$Re \equiv \frac{\rho \bar{u}_x h}{\mu}, \tag{19}$$

exceeds about 1150 (de Marsily, 1986, p. 66). The Reynolds number is a dimensionless measure of the relative strengths of inertial forces to viscous forces. At low Reynolds numbers, viscous forces are strong enough to damp out any perturbations from the uni-directional, laminar flow field, whereas at sufficiently high velocities small perturbations to the laminar flow field will tend to grow in an unstable manner. Combining eqs. (13) and (19) yields the following criterion for the laminar solution derived in the previous section to be *stable*:

$$|\overline{\nabla p}| < \frac{13800\mu^2}{\rho h^4}. \tag{20}$$

This expression shows that high viscosity, low density, and small apertures all tend to stabilize the flow field.

The stability condition given by eq. (20) is satisfied in most subsurface flow situations. For example, consider water with a viscosity of 10^{-3} Pa·s and a density of 10^3 kg/m^3. Even for fracture apertures as large as 10^{-3} m, laminar flow will be stable for pressure gradients as high as about 1.4×10^7 Pa/m. This gradient is equivalent to about 140 bars/m, which is much larger than the gradients that would typically be encountered. If the fluid is air, with a viscosity of about 2×10^{-5} Pa·s and a density of about 1.2 kg/m^3 (Batchelor, 1967, p. 175), then flow through a 1 mm wide fracture will be stable for pressure gradients up to about 4.6×10^6 Pa/m, or about 46 bars/m. Hence, it seems that genuine turbulent instability can often be ignored when studying flow through rock fractures. Possible exceptions include situations of forced fluid flow, such as hydraulic fracturing (Jung, 1989), where large pressure gradients may be developed. For a real rough-walled fracture, however, inertia effects due to tortuous flowpaths will lead to deviations from the cubic law long before genuine turbulence occurs, i.e., at lower flowrates, as will be discussed below.

Reynolds Lubrication Approximation

At low flowrates, the two main causes of deviations from the cubic law are roughness of the fracture walls, which leads to spatial variations in aperture, and asperity contact between the opposing fracture faces, which leads to partial obstruction of the flow. Although asperity contact can be thought of as an extreme case of aperture variation, it is convenient to analyze these two effects separately. First consider the case where the aperture varies from point to point, but is always greater than zero, i.e., no asperity contact. Under certain geometric and kinematic conditions, the Navier-Stokes equations can be reduced to the simpler Reynolds ''lubrication'' equation. One requirement for the Reynolds equation to be valid is that viscous forces dominate the inertial forces (Batchelor, 1967, p. 222). To quantify this criterion, we first estimate the orders of magnitude of the three terms appearing in eq. (5). The first term, $\mu \nabla^2 \mathbf{u}$,

represents the viscous forces; the second term, $\rho(\mathbf{u}\cdot\nabla)\mathbf{u}$, represents inertial forces; and the third term, ∇p, represents the pressure gradient. Let U be a characteristic magnitude of the velocity, which could be thought of as the average velocity, as in eq. (13), although a precise definition is not needed for an order-of-magnitude analysis. Across the thickness of the fracture, the velocity varies from 0 at the upper and lower walls to some maximum value which is on the order of U, and this variation occurs over a distance h. Hence the order of magnitude of the viscous terms can be estimated to be

$$mag\,[\mu\nabla^2\mathbf{u}] \approx \frac{\mu U}{h^2}, \tag{21}$$

where h^2 appears due to the fact that there are two derivatives taken with respect to z in the expression $\nabla^2\mathbf{u}$. The magnitude of the pressure gradient term can be estimated to be

$$mag\,[\nabla p\,] \approx |\overline{\nabla p}\,|, \tag{22}$$

where $|\overline{\nabla p}\,|$ is the magnitude of the *overall* reduced pressure gradient established at the ends ends of the fracture, as in Fig 1. To check that this sort of order-of-magnitude analysis is sensible, note that equating the magnitudes of the viscous forces and the pressure gradient from eqs. (21) and (22) leads to the following estimate for the characteristic velocity U:

$$mag\,[U] \approx \frac{|\overline{\nabla p}\,|h^2}{\mu}, \tag{23}$$

which is consistent with the form that was calculated (exactly) for the parallel plate

model, eq. (10).

We now estimate the magnitude of the inertial forces. First note that the magnitudes calculated above correspond to the forces acting *in the direction of the mean flow*. This is clear for the term ∇p, which acts in this direction. For the viscous term, this is seen by noting that U is actually the characteristic velocity in the x direction, parallel to the applied macroscopic pressure gradient. To estimate the magnitude of the term $(\mathbf{u}\cdot\nabla)\mathbf{u}$, we first define a characteristic length Λ in the x direction, which may be the wavelength of the aperture variations, or the distance between asperity obstacles, etc. (see Fig. 2). The velocity gradient is then on the order of U/Λ, and the inertial terms have magnitude

$$mag\,[(\mathbf{u}\cdot\nabla)\mathbf{u}] \approx \frac{\rho U^2}{\Lambda}. \tag{24}$$

For the inertia terms to be smaller than the viscous terms, we must have (Schlichting, 1968, p. 109)

$$\frac{\rho U^2}{\Lambda} \ll \frac{\mu U}{h^2}, \qquad \text{or} \quad Re^* \equiv \frac{\rho U h^2}{\mu \Lambda} \ll 1, \tag{25}$$

where the reduced Reynolds number Re^* is defined to be the product of the traditional Reynolds number, $\rho Uh/\mu$, and the geometrical parameter h/Λ. The question of whether or not this condition is satisfied in typical subsurface flow situations will be discussed below.

If condition (25) is satisfied, then the advective inertia term $(\mathbf{u}\cdot\nabla)\mathbf{u}$ is negligible compared to the other two terms in eq. (5), and we can replace the Navier-Stokes equations (1) with the Stokes "creeping flow" equations:

$$\mu \nabla^2 \mathbf{u} = \nabla p \ , \tag{26}$$

which can be written out in component form as

$$\frac{\partial^2 u_x}{\partial x^2} + \frac{\partial^2 u_x}{\partial y^2} + \frac{\partial^2 u_x}{\partial z^2} = \frac{1}{\mu}\frac{\partial p}{\partial x}, \tag{27a}$$

$$\frac{\partial^2 u_y}{\partial x^2} + \frac{\partial^2 u_y}{\partial y^2} + \frac{\partial^2 u_y}{\partial z^2} = \frac{1}{\mu}\frac{\partial p}{\partial y}, \tag{27b}$$

$$\frac{\partial^2 u_z}{\partial x^2} + \frac{\partial^2 u_z}{\partial y^2} + \frac{\partial^2 u_z}{\partial z^2} = \frac{1}{\mu}\frac{\partial p}{\partial z}. \tag{27c}$$

These three equations must still be accompanied by the continuity equation, (11). The Stokes equations are linear, which makes them easier to solve than the Navier-Stokes equations. Another slight operational advantage to their use is that there is a uniqueness theorem for solutions to the Stokes equations in finite regions such as the space between two fracture walls (see Langlois, 1964, pp. 161-163). This is of course a purely mathematical consequence of ignoring the inertia terms, which are the source of turbulence. The Stokes equations are nevertheless three-dimensional, in general. For the parallel plate model, the equations effectively become one-dimensional, since there is only one nonzero velocity component, and it depends on only one position coordinate. Any deviation from the parallel plate geometry causes the velocity vector to have at least two nonzero components, which depend on at least two of the position coordinates. Although the linearity of the Stokes equations allows methods such as Green's functions (Pozrikidis, 1987,1992) and separation of variables (Lee and Fung, 1969; Tsay and Weinbaum, 1991) to be used, solutions are still difficult to obtain, and

unwieldy to utilize and interpret. Hence, it is desirable to further simplify the equations before attempting to solve them for different types of fracture geometries.

The validity of the Stokes equations requires that the flow rate (as quantified by the reduced Reynolds number) be sufficiently small. Further reduction to the simpler Reynolds lubrication equation requires the additional criterion that changes in aperture occur gradually. To derive the lubrication equations, we first assume that the characteristic wavelength of aperture variations, Λ, is much larger than the aperture h. Using an order-of-magnitude analysis similar to that which is commonly used to derive the boundary-layer equations (Schlichting, 1968, pp. 118-119), the magnitudes of the second derivatives of u_x that appear in eq. (27) can be estimated as

$$mag\left[\frac{\partial^2 u_x}{\partial x^2}\right] \approx mag\left[\frac{\partial^2 u_x}{\partial y^2}\right] \approx \frac{U}{\Lambda^2}, \qquad mag\left[\frac{\partial^2 u_x}{\partial z^2}\right] \approx \frac{U}{h^2}, \tag{28}$$

where we assume that the characteristic lengths in the x and y directions are the same for a macroscopically isotropic fracture. Eq. (28) shows that if $(h/\Lambda)^2 \ll 1$, the derivatives with respect to x or y will be negligible compared to those with respect to z.

The proper choice of a characteristic magnitude for u_y is not as clear, since, for example, the average of u_y taken over the entire fracture plane must be zero. This follows from the fact that for a macroscopically isotropic fracture, if the overall pressure gradient points in the x direction, the overall flux must also have no y component (see Bear, 1972, p. 142; Phillips, 1991, p. 27). Whatever value is used for the characteristic magnitude of u_y, the conclusion will nevertheless follow that the $\partial^2 u_y/\partial z^2$ is the dominant term on the left side of eq. (27b), as long as $h/\Lambda \ll 1$. Although the average value of $\partial p/\partial y$ is also zero, local variations in aperture will cause this term to be locally nonzero; as it is the only term on the right-hand side of eq. (27b), $\partial p/\partial y$ cannot be ignored.

Estimates of the magnitudes of the terms appearing in eq. (27c) are more difficult to make. The argument that was made above in the solution of the parallel plate problem was that since u_z must vanish at the top and bottom walls of the fracture, and since the average value of u_z must vanish over the entire fracture plane, then u_z will be small everywhere, and can be neglected. This argument does not actually prove, however, that u_z will be nearly zero *locally* at each point (x,y,z). The assumption that u_z is negligible seems plausible if the aperture variations are very gradual, i.e., $h/\Lambda \ll 1$. But as long as the fluid always fills the entire fracture, this assumption can never be exactly true, except in the case of uniform aperture (i.e., parallel plate flow). Abrupt changes in aperture in the x or y direction would certainly require that the fluid velocity have an appreciable component in the z direction. More precise estimates of the range of validity of this particular assumption will be discussed in the next section. For now, we assume that u_z is negligible.

According to the order-of-magnitude arguments given above, if the aperture varies gradually in the plane of the fracture, the Stokes equations (27a-c) can be replaced by

$$\mu \frac{\partial^2 u_x}{\partial z^2} = \frac{\partial p}{\partial x}, \tag{29a}$$

$$\mu \frac{\partial^2 u_y}{\partial z^2} = \frac{\partial p}{\partial y}. \tag{29b}$$

These equations have the same form as eq. (9a), which occurred in the parallel plate model, although now the velocity components vary with $x, y,$ and z, and the pressure gradient will in general vary with x and y. Since u_z was assumed to vanish, $\partial p/\partial z$ must be zero in order to be consistent with eq. (27c). The right-hand sides of eq. (29) do not depend on z, so the equations can be integrated with respect to z, bearing in

mind the no-slip boundary conditions at the top and bottom walls, $z = h_1$ and $z = -h_2$ (see Fig. 2), to yield

$$u_x(x,y,z) = \frac{1}{2\mu}\frac{\partial p(x,y)}{\partial x}(z-h_1)(z+h_2), \tag{30a}$$

$$u_y(x,y,z) = \frac{1}{2\mu}\frac{\partial p(x,y)}{\partial y}(z-h_1)(z+h_2), \tag{30b}$$

which is essentially the same parabolic profile as was found for the case of constant aperture, eq. (10), except that the velocity is now parallel to the local pressure gradient, which may not always be aligned with the overall pressure gradient. If we do not assume that the two fracture walls are symmetric with respect to the z axis, the two half-apertures $h_1(x,y)$ and $h_2(x,y)$ will not necessarily be equal.

As we are ultimately interested in the total flux through the fracture, we now integrate the velocity profiles given by eq. (30) across the width of the fracture, from $-h_2$ to h_1, to find

$$\overline{u}_x = \frac{1}{h}\int_{-h_2}^{h_1} u_x(x,y,z)\,dz = \frac{-h^3(x,y)}{12\mu}\frac{\partial p(x,y)}{\partial x}, \tag{31a}$$

$$\overline{u}_y = \frac{1}{h}\int_{-h_2}^{h_1} u_y(x,y,z)\,dz = \frac{-h^3(x,y)}{12\mu}\frac{\partial p(x,y)}{\partial y}, \tag{31b}$$

where the overbar indicates an average taken over the z coordinate, and the total aperture is given by $h = h_1 + h_2$. Evaluation of the integrals in eq. (31) is facilitated by

defining a new variable $\zeta = z + h_2$ that represents the distance along the z axis from the bottom wall.

Eqs. (31a,b) represent an approximate solution to the equations of conservation of momentum, eq. (29), but still contain an unknown pressure field. The pressure is found by utilizing the continuity equation, in some form. The continuity equation as given by eq. (2), however, applies to the actual local velocities, not to the integrated values. But $\nabla \cdot \mathbf{u} = 0$, so the integral of $\nabla \cdot \mathbf{u}$ with respect to z must also be zero. Interchanging the order of these two operations then shows that the divergence of the average velocity, $\bar{\mathbf{u}}$, is also equal to zero. (In general, the order of these two mathematical operations can be interchanged as long as the velocity components vanish at $z = h_1$ and $z = -h_2$, as can be proven by applying Liebnitz' rule for differentiating and integral with respect to a parameter). Hence, we can apply eq. (2) to the profiles given in eq. (29), yielding

$$\nabla \cdot [h^3(x,y) \nabla p(x,y)] = 0 , \tag{32a}$$

$$i.e., \quad \frac{\partial}{\partial x}\left[h^3(x,y)\frac{\partial p}{\partial x}\right] + \frac{\partial}{\partial y}\left[h^3(x,y)\frac{\partial p}{\partial y}\right] = 0 , \tag{32b}$$

which is the equation first derived by Reynolds (1886) for lubrication-type flows. Eq. (32) has often been derived in the context of studying fracture permeability (see Walsh, 1981; Brown, 1989), by merely assuming that the cubic law holds *locally* at each point in the fracture, and then invoking the principle of conservation of mass. Although this is a useful interpretation of eq. (32), this type of derivation does not clearly display the conditions necessary for the validity of the various approximations that are implicitly contained in the final equation.

Eq. (32) is a single, linear partial differential equation that describes the pressure field in the fracture plane. Its solution requires prescription of either the pressures or their normal derivatives (i.e., the fluxes) over the outer boundary of the fracture plane. To use this equation to find the permeability of a fracture, one would typically solve it in a rectangular region defined by $0<x<L_x$, $0<y<L_y$. The two lateral sides $y=0$ and $y=L_y$ would be no-flow boundaries, whereas the sides $x=0$ and $x=L_x$ are constant pressure boundaries. If there is no flow out of the two lateral sides, $\bar{u}_y$ must equal 0 at $y=0$ and $y=L_y$. Eq. (31) shows that $\bar{u}_y$ is proportional to $\partial p/\partial y$, so we see that the normal derivative of the pressure must vanish on the lateral boundaries. The $x=0$ boundary would have $p=p_i$, and the $x=L_x$ boundary would have $p=p_o$, where $(p_o-p_i)/L_x=\overline{\nabla p}$. The overall flux would be found by integrating $\bar{u}_x$ across the $x=0$ inlet of the fracture:

$$Q = \int_{y=0}^{y=L_y} \bar{u}_x(0,y)dy \,. \tag{33}$$

Finally, the fracture transmissivity would be found from $T = Q\mu/|\overline{\nabla p}|$. A fracture permeability could be defined as in eq. (16) by dividing T by the nominal area of the fracture, $w<h>$, although the transmissivity is the more generally useful parameter, as its definition does not require knowledge of the mean aperture.

Range of Validity of the Lubrication Approximation

Reduction of the Navier-Stokes equations to the Reynolds equation requires that the aperture h always be much less, in some sense, than the characteristic spatial wavelength Λ of the aperture variations. It would be useful to have a quantitative measure of how small h/Λ must be in order for the solutions to the Reynolds equation to closely approximate the solutions to the Navier-Stokes equations. Strict *a priori*

error estimates are unfortunately difficult to derive. A more practical approach is to focus on a specific geometry for which analytical treatment of the Navier-Stokes equations is possible, so as to allow comparison with the lubrication theory predictions. For instance, consider the problem of flow between a smooth wall and a sinusoidally-varying wall, such as the geometry shown in Fig. 3. The aperture can be described by

$$h(x) = \langle h \rangle [1 + \delta \sin(2\pi x/\lambda)] \,, \tag{34}$$

where λ is the wavelength of the aperture variations, and δ is the relative amplitude of the aperture variations, normalized with respect to $\langle h \rangle$. The aperture does not vary with y, and the flow is in the x direction.

Hasegawa and Izuchi (1983) performed a perturbation analysis of this problem, using as their small parameters the Reynolds number, $Re = \rho U \langle h \rangle / \mu$, where U is the mean velocity that would occur if the walls were smooth, and the geometrical parameter $\varepsilon = \langle h \rangle / \lambda$. The velocity components u_x and u_z are nonzero, and are functions of x and z. Following the standard procedure of regular perturbations, Hasegawa and Izuchi (1983) essentially assumed that u_x and u_z could be expanded as power series in Re and ε, inserted these expansions into the Navier-Stokes equations, and then equated the coefficients of each power of Re and ε to zero. This approach reduces the nonlinear Navier-Stokes equations to a sequence of linear equations. The zeroth-order solution, corresponding to $Re = 0$ and $\varepsilon = 0$, is identical to the corresponding solution of the lubrication equation for this geometry. Hasegawa and Izuchi (1983) also found the first-order correction due to non-zero values of Re and ε. These corrections represent the errors incurred by replacing the Navier-Stokes equations with the Reynolds lubrication equation.

When translated into the present notation, the solution found by Hasegawa and Izuchi, including the first non-trivial corrections in Re and ε, can be expressed as (see

their eqs. 27-32)

$$h_H^3 = \langle h^{-3} \rangle^{-1} \left[1 - \frac{3\pi^2(1-\delta^2)\delta^4}{5(1+\delta^2/2)} \left[1 + \frac{13}{8085} Re^2 \right] \varepsilon^2 \right] . \qquad (35)$$

The harmonic mean $\langle h^{-3} \rangle^{-1}$ would result from solving a one-dimensional version of the lubrication equation (see eq. (42) below). The second term in brackets therefore represents the discrepancy between the Navier-Stokes and Reynolds solutions. To see the conditions that must be satisfied by *Re* and ε in order for this term to be negligible, first let $Re=0$. As δ is restricted by definition to lie between 0 and 1, the term that multiplies ε^2 in eq. (35) is always less than 0.662. In order for the error to be less than, say, 10%, we would need $0.662\langle h \rangle^2/\lambda^2 < 0.1$, which implies $\lambda > 2.57\langle h \rangle$. Since the aperture undergoes its maximum variation within a half-wavelength, this condition is roughly equivalent to saying that sizable aperture variations can only occur over distances greater than the mean aperture $\langle h \rangle$, for the Reynolds solution to be valid. As pointed out by Zimmerman et al. (1991), this condition is much less restrictive than the one proposed earlier by Brown (1987), which can, in the present context of a sinusoidal aperture variation, be expressed as $\lambda > 30\langle h \rangle$. Nevertheless, examination of aperture profiles measured on real rock fractures (Gentier et al., 1989) shows that even this less restrictive condition is not always satisfied.

We now consider the criteria that must be met by *Re* in order for the correction term in the solution found by Hasegawa and Izuchi (1983) to be small. The term due to nonzero *Re* in eq. (35) is always multiplied by the term due to nonzero $\langle h \rangle/\lambda$. As we have already seen that the Reynolds approximation will break down if λ is not sufficiently small, in order to find restrictions on the allowable values of *Re* we now restrict our attention to the worst admissible case, $\lambda = 2.57\langle h \rangle$, in which case the error is already 10% when $Re=0$. If we now assume that at most another 10% error will be

tolerated, eq. (35) yields the condition $13Re^2/8085 < 1$, which in turn implies $Re < 25$. However, when $Re > 1$, it is not necessarily permissable to ignore the subsequent terms in the perturbation series, which would be proportional to higher powers of Re, but which were not calculated by Hasegawa and Izuchi. What can be said with some confidence based on eq. (35) is that if $Re < 1$, for example, the error due to a nonzero Reynolds number will be smaller than that due to nonzero $<h>/\lambda$. Hence $Re < 1$ seems to be a conservative criterion for the lubrication equation to provide a reasonable approximation to the Navier-Stokes equations, for this particular problem.

When expressed in terms of parameters such as the applied pressure gradient, this criterion takes a form similar to that given in eq. (20) for the flow to be stable, except that the maximum Reynolds number is 1 instead of 1150:

$$|\overline{\nabla p}| < \frac{12\mu^2}{\rho h^4}. \tag{36}$$

The condition for the flow to be governed by the Reynolds lubrication equation is therefore stricter, by about a factor of one thousand, than the condition that the flow (in a smooth-walled channel) be laminar. Following the analysis given above for the onset of turbulence, we see that for a fracture having an aperture of 1 mm, saturated with water of density 1000 kg/m^3 and viscosity 0.001 Pa·s, the pressure gradient must be less than 10^4 Pa/m, or about 0.1 bars/m. This critical gradient is certainly larger than most naturally-occurring groundwater potential gradients, but could be exceeded in cases of forced flow (cf., Jung, 1989).

The criterion given by eq. (36) does not merely refer to the validity of the lubrication equation as an acceptable mathematical expediency. More fundamentally, this condition also determines whether or not the flow process will be linear or nonlinear. If this and the previously-defined geometrical criteria are satisfied, the term involving

Re will be negligible, so h_H will be independent of the flowrate, which in turn implies (see eqs. 14,18) that the flowrate will be directly proportional to the applied pressure gradient. For larger values of Re, eq. (35) shows that h_H will depend on the pressure gradient, in which case eqs. (14,18) show that the flowrate will be a nonlinear function of $|\overline{\nabla p}|$. Comparison of eq. (36) and eq. (20) shows that the appearance of a nonlinear relationship between Q and $\overline{\nabla p}$ can occur at flowrates that are much less than those required to produce genuine turbulence. This point was made by Bear (1972, p. 178) in the context of flow through three-dimensional porous media. Bear discussed experimental results by Wright (1968) and others that showed nonlinear effects arising at Reynolds numbers as low as 1–10, whereas true turbulence did not occur until Re reached about 60–100. Geertsma (1974) pointed out, also in the context of three-dimensional porous media, that in cases of practical importance in petroleum engineering, including converging flow near wellbores, nonlinear departures from Darcy's law occur during laminar, not turbulent, flow. Coulaud et al. (1991) performed numerical solution to the full Navier-Stokes equations for transverse flow past an array of infinitely long, parallel cylinders, and found slight nonlinearity in the relationship between pressure drop and flowrate to begin at about $Re=2$, although the flow was still clearly laminar. Nevertheless, deviations from a Darcy-type linear relationship between $\overline{\nabla p}$ and Q are often attributed, perhaps erroneously, to turbulence (cf., Geertsma, 1974).

Numerical Solutions to the Lubrication Equations

Under the conditions that the reduced Reynolds number is small, and that the aperture variations occur gradually, flow through a fracture can be described by the lubrication equation, eq. (32). Although it is in one sense simpler than either the Navier-Stokes or Stokes equations, because it is a single scalar equation rather than a vector equation, the presence of the term $h(x,y)$ renders it an equation with variable

coefficients. For certain special (anisotropic) geometries the equation becomes one-dimensional, in which case it is easy to solve; these cases are discussed in the next section. For arbitrary isotropic aperture distributions it cannot be solved analytically, but it is amenable to numerical solution procedures. Several studies have been done in which the equations were solved numerically for various aperture distributions, with the intention of finding some simple relation between the transmissivity and the statistics of the aperture distribution.

Patir and Cheng (1978) used finite differences to solve the lubrication equation for flow between two surfaces, the half-apertures of which, h_1 and h_2, obeyed a Gaussian height distribution with linearly-decreasing auto-correlation functions. Although their intended application was to lubrication flows in machine components, it is convenient to use the terminology of fracture flow when discussing their results. They studied both statistically isotropic fractures, and anisotropic fractures with aperture distributions that had different correlation lengths in two orthogonal directions; only the results for isotropic fractures will be discussed here. As the transmissivity of a fracture is proportional to the cube of the hydraulic aperture, as shown by eq. (18), the numerically-calculated transmissivities can be discussed in terms of the hydraulic aperture, h_H.

Patir and Cheng (1978) displayed their calculated results as a function of the ratio of the nominal aperture h_o to the standard deviation of the roughness distribution function, σ_d; the meanings of these parameters are discussed in more detail below. The results are shown in Fig. 4, in which each data point represents the average of about ten different realizations based on the same values of h_o and σ_d. No values were given for the correlation lengths of the height distributions, although they were presumably much less than the overall length L of the computational region, and greater than the length l used in the finite difference calculations. For values of h_o/σ_d between 0.5 and 6.0, Patir and Cheng found that the hydraulic aperture could be fit

with the function (see Fig. 4)

$$h_H{}^3 = h_o^3 \left[1 - 0.90\, e^{-0.56 h_o/\sigma_d}\right] . \tag{37}$$

According to these results, the nominal aperture h_o is a zeroth-order approximation to the hydraulic aperture h_H. The effect of surface roughness is to decrease the hydraulic aperture below the value h_o. Although eq. (37) provides a reasonable fit to the data when h_o/σ_d lies between 0.5 and 6, the parameters in the equation were *not* chosen so as to provide a best fit in the limit as $h_o/\sigma_d \rightarrow \infty$; hence, this equation should not be thought of as a rigorous first-order correction to the cubic law in the limit of small amounts of roughness.

An important point to note about the findings of Patir and Cheng concerns the issue of contact areas at which the two opposing surfaces touch, and the manner in which this affects the definitions of h_o and σ_d. Translated into the present notation, they defined upper and lower surfaces, the distances of which from the $z = 0$ plane are given by two half-aperture distributions as follows:

$$h_1(x,y) = \frac{h_o}{2} + d_1(x,y) , \tag{38a}$$

$$h_2(x,y) = \frac{h_o}{2} + d_2(x,y) , \tag{38b}$$

where the functions $d_i(x,y)$ have a mean value of zero. If $h_1 + h_2 > 0$, then the fracture is open at that point, and the aperture is given by $h = h_1 + h_2$. However, if $h_1 + h_2 \leq 0$, i.e., the curves representing the upper and lower surfaces of the fracture

overlap each other, then the fracture is assumed to be obstructed at that point, and the aperture is taken to be zero. As pointed out by Brown (1989), the mean aperture $<h>$ will equal h_o if there are no contact regions, but $<h>$ will be greater than h_o if there are contact regions, since the negative values of the function $h = h_1 + h_2$ are not allowed to contribute to the calculation of $<h>$. Hence, the parameters h_o and σ_d used by Patir and Cheng (1978) do not represent the actual mean and standard deviation of the aperture, except for small values of σ_d, when no contact occurs. According to Patir and Cheng, contact regions occurred when $h_o/\sigma_d < 3$, but they did not quantify the amount of contact area that occurred. Therefore, when $h_o/\sigma_d < 3$, the results shown in eq. (37) and Fig. 4 represent the combined effects of aperture variation *and* asperity contact.

Brown (1987,1989) performed a similar finite difference analysis of the Reynolds equation, for fractures having randomly-generated, *fractal* roughness profiles. The fractal dimension of the fracture walls varied from 2.0, which represents a smooth wall, to 2.5, which was found by Brown and Scholz (1985) to correspond to a maximum amount of roughness that occurs for real rock fractures. The flow region between fracture walls was formed by generating two surfaces having the same fractal dimension, and then choosing a value for the nominal aperture h_o, which is the mean distance between the two planes. The aperture was then set to zero at any point in the fracture plane where the two fracture walls overlapped. Although Brown presented most of his results in terms of the actual mean aperture $<h>$, he followed Patir and Cheng (1978) in using σ_d to quantify the roughness, which is to say, he used the standard deviation of the distance that exists between the two surfaces *before* all negative apertures are set to zero. Hence, it is not possible to replot his data in terms of the actual mean and standard deviation of the *fracture aperture*; this definition of σ_d must be kept in mind when examining Brown's results.

Fig. 4 also shows the transmissivities that were computed by Brown (1987) for a surface having a fractal dimension of 2.5, normalized to the cubic law value based on the mean aperture. Each one of the data points represents the mean of ten different realizations. Brown found that the fractal dimension had little effect on the computed transmissivities, and that h_H seemed to be mainly a function of $<h>$ and σ_d. Brown's mean transmissivities fell very close to the values found by Patir and Cheng (1978), regardless of the fractal dimension of the surface. This agreement provides some validation of the computational procedures used in the two studies. However, for low values of $<h>/\sigma_d$, the unquantified amount of contact area makes it difficult to rigorously compare the two sets of results, since h_o and $<h>$ are not equivalent when there is contact between the two fracture faces.

Analytical Treatment of the Lubrication Model

Once the Navier-Stokes equations have been reduced to the Reynolds lubrication equation (32), fluid flow through the fracture is then governed by the very same equation that governs, say, heat conduction in an isotropic but inhomogeneous two-dimensional medium. The cube of the local aperture, $h^3(x,y)$, plays the same role as the thermal conductivity, k, aside from the multiplicative constant 1/12 which can be factored out and ignored. A similar equation governs porous medium flow in a nearly-horizontal aquifer which has a permeability and/or thickness that varies gradually from point to point (Bear, 1972, p. 215). The problem of finding the effective hydraulic aperture for a fracture that is governed by the Reynolds equation is therefore equivalent to finding the effective conductivity of a heterogeneous two-dimensional conductivity field, be it electrical, thermal, or hydraulic. A great deal of mathematical work has been done on this problem, the results of which can be applied directly to fracture flow, with the understanding that if the aperture (i.e., conductivity) varies too rapidly, in the sense quantified previously, the Reynolds equation will no longer be

valid.

The effective macroscopic conductivity of a heterogeneous medium depends not only on the statistical distribution of the local conductivities, but also on the geometrical and topological manner in which the local conductivity is distributed. In other words, the spatial correlation between the regions of high and low conductivity also has an effect on the overall conductance. However, if the statistical distribution of conductances is known, but the correlation structure of the conductivity field is either unknown or ignored, upper and lower bounds can be computed for the overall effective conductivity (Beran, 1968, p. 242; Dagan, 1979). These bounds, which are derived using variational principles and certain trial functions for the local pressure field, can be expressed as

$$<\frac{1}{k}> \leq k_{eff} \leq <k>, \tag{39a}$$

$$\text{or} \quad <h^{-3}>^{-1} \leq h_H^3 \leq <h^3>, \tag{39b}$$

where we identify the local conductivity with h^3. The lower bound $<1/k>$ is often called the harmonic mean, whereas the upper bound $<k>$ is called the arithmetic mean (de Marsily, 1986, p. 81).

The upper bound can be thought of as corresponding to the hypothetical situation in which all of the conductive elements are arranged in parallel with each other, whereas the lower bound corresponds to a series arrangement of the individual elements (Dagan, 1979). These extreme cases correspond to geometries in which the aperture varies in only one of the two directions, x or y, while the imposed pressure gradient is in the x direction (see Fig. 5). For example, in the case where the aperture varies only in the direction of the applied pressure gradient, the Reynolds equation

(32) reduces to the one-dimensional form

$$\frac{d}{dx}\left[h^3(x)\frac{dp}{dx}\right]=0, \tag{40}$$

which can be integrated once to yield

$$h^3(x)\frac{dp}{dx}=C\ , \tag{41}$$

where C is a constant of integration. Comparison of eqs. (41) and (31a) shows that the constant of integration is equal to $-12\mu\bar{u}_x$. A second integration from $x=0$ to $x=L_x$ yields

$$p_o-p_i=-12\mu\bar{u}_x\int_0^{L_x}\frac{dx}{h^3(x)}=-12\mu\bar{u}_xL_x\langle h^{-3}\rangle\ , \tag{42}$$

which can be rearranged to yield

$$\bar{u}_x=\frac{-|\overline{\nabla p}|}{12\mu}\langle h^{-3}\rangle^{-1}. \tag{43}$$

The total flux is found by integrating $\bar{u}_x$ in the y-direction, as in eq. (33), which yields

$$Q=\frac{-|\overline{\nabla p}|L_y}{12\mu}\langle h^{-3}\rangle^{-1}. \tag{44}$$

But L_y is equivalent to w, the width of the fracture in the direction normal to the flow, so comparison with eqs. (12,18) shows that this model leads to

$$h_H^3 = <h^{-3}>^{-1}, \tag{45}$$

which is identical to the lower bound in eq. (39). An analogous treatment of the case where the aperture varies only in the direction normal to the flow would lead to (see Neuzil and Tracy, 1981)

$$h_H^3 = <h^3>, \tag{46}$$

which reproduces the upper bound. These models have been used as heuristic devices to estimate the effect of aperture variations on the overall conductivity (see Neuzil and Tracy, 1981; Silliman, 1989). However, it must be understood that these types of aperture variations do not lead to macroscopically isotropic behavior. Hence, rather than interpret the bounds given by eq. (39) as representing any specific simplified fracture geometry, we interpret these "series" and "parallel" conductances as upper and lower bounds that utilize information about the aperture distribution function of the fracture, but do not utilize information concerning the spatial correlation of the aperture field.

More restrictive upper and lower bounds on the overall effective conductivity of a heterogeneous medium have been found by Hashin and Shtrikman (1962). For the commonly-assumed case of a log-normal distribution of conductivities, however, these bounds degenerate (Dagan, 1979) into the series and parallel bounds given by eq. (39a). For this case, the "self-consistent field" approximation has been used (Dagan, 1979), along with a perturbation approach (Dagan, 1993), to approximate the effective

conductivity in terms of the mean and standard deviation of the conductivity distribution function. In the case of a statistically-isotropic $m-$dimensional media, Dagan found

$$k_{eff} = <k> e^{-\sigma_Y^2/2} \left[1 + \left[\frac{1}{2} - \frac{1}{m} \right] \sigma_Y^2 + \left[\frac{1}{2} - \frac{1}{m} \right]^2 \frac{\sigma_Y^4}{2} + \cdots \right], \tag{47}$$

where $Y = \ln(k)$, and σ_Y is the standard deviation of $\ln(k)$. The term outside of the square brackets is equal to the *geometric mean* of the conductivity distribution, k_G, which is defined (in general) by

$$k_G = e^{<\ln(k)>}. \tag{48}$$

As a fracture is analogous to a two-dimensional conductivity field, the appropriate value of m is 2, in which case the σ_Y^2 and σ_Y^4 terms inside the brackets drop out, leaving

$$k_{eff} = <k> e^{-\sigma_Y^2/2} + O(\sigma_Y^6). \tag{49}$$

This result can also be expressed as

$$k_{eff} = <k> \left[1 - \frac{\sigma_Y^2}{2} + \cdots \right]. \tag{50}$$

Although eq. (50) was derived for the specific case of a lognormal conductivity distribution, it can nevertheless be used *as an approximation* regardless of the form of the conductivity distribution. For this purpose, it would be convenient to express eqs. (49,50) in terms of the standard deviation of k, rather than in terms of the standard deviation of $\ln(k)$. To do this, we first recall that if k is lognormally distributed, then the first two moments of k are related to the first two moments of $y = \ln(k)$ by (Aitchison and Brown, 1957, p. 11)

$$<k> = e^{<Y> + \sigma_Y^2/2}, \tag{51}$$

$$\sigma_k^2 = <k>^2 \left[e^{\sigma_Y^2} - 1 \right]. \tag{52}$$

Eliminating σ_Y^2 from eqs. (49,52) yields

$$k_{eff} \approx <k> \left[1 + \frac{\sigma_k^2}{<k>^2} \right]^{-1/2}, \tag{53}$$

which, to first-order in σ_k^2, can be expressed as

$$k_{eff} \approx <k> \left[1 - \frac{1}{2} \frac{\sigma_k^2}{<k>^2} + \cdots \right]. \tag{54}$$

Eq. (54) agrees with the result that can be found from a two-dimensional version of the calculation performed by Landau and Lifshitz (1960, pp. 45-46), who assumed that the conductivity varied smoothly in space about its mean value, $<k>$, but did not assume that k was lognormally distributed. It therefore is a valid approximation, up to

order σ_k^2, for all smoothly-varying two-dimensional conductivity distributions. Since smooth spatial variation is a necessary condition for the use of the lubrication approximation, this result holds in all cases for which the lubrication approximation applies.

We now make use of the identification of k with h^3 to express the above results in terms of the moments of the aperture distribution itself. In general, for arbitrary aperture distributions, there is no fixed relationship between $<h^3>$ and $<h>$, or between σ_k^2 and σ_h^2. In the case of a lognormal distribution, however, we can make use of the fact that $\ln(k)=\ln(h^3)=3\ln(h)$ to find that $<\ln(k)>=3<\ln(h)>$, and $\sigma_{\ln k}^2=9\sigma_{\ln h}^2$ (Aitchison and Brown, 1957, p. 11). Furthermore, if k is lognormally distributed, then so is $h=k^{1/3}$. If we let $z=\ln(h)$, where z has mean value $<z>$ and variance σ_z^2, then the statistical moments $<h^n>$ are given by (Aitchison and Brown, 1957, p. 8; Gutjahr et al., 1978)

$$<h^n> = e^{n<z>+n^2\sigma_z^2/2}. \tag{55}$$

Using these relationships, along with eqs. (51,52), we can rewrite eqs. (53,54) as

$$h_H^3 \approx <h^3>\left[1+\frac{9\sigma_h^2}{<h>^2}\right]^{-1/2} \approx <h^3>\left[1-\frac{9\sigma_h^2}{2<h>^2}+\cdots\right]. \tag{56}$$

Again using eqs. (51,52), with h in place of k and $z=ln(h)$ in place of $y=ln(k)$, we find after some algebra that eq. (56) can also be written as

$$h_H^3 \approx <h>^3\left[1-\frac{3}{2}\frac{\sigma_h^2}{<h>^2}+\cdots\right]. \tag{57}$$

Eq. (57) indicates that when there is roughness, the hydraulic aperture is smaller than the mean aperture. This is a non-trivial result since, for example, it can be shown (see Silliman, 1989) that the lower bound on h_H given by eq. (39b) can never exceed $<h>$, whereas the upper bound can never be less than $<h>$. Hence, the bounds in themselves are not powerful enough to show that $h_H \leq <h>$. Eq. (57) is also in rough agreement with the numerical results of Patir and Cheng (1978) and Brown (1987), particularly when $h/\sigma > 2$, which is the range where, due to lack of substantial contact area, the various definitions used for h and σ coincide.

Eq. (57) has also been derived by other methods, using specific fracture geometries that did not require lognormal aperture distributions. Elrod (1979) used Fourier transforms to solve the Reynolds equation for a ''fracture'' the aperture of which had ''sinusoidal ripples in two mutually perpendicular directions'', and arrived at eq. (57) for the isotropic case. Zimmerman et al. (1991) considered the case of small regions of uni-directional ripples, as in eq. (34), which were then assembled together so that the direction of striation was randomly distributed. For both sinusoidal and sawtooth profiles, their results agree with eq. (57) up to terms of order $\sigma_h^2/<h>^2$. They also examined the effect of higher-frequency sinusoidal components in the aperture profile, using the assumption that the amplitudes of the sinusoidal components were positively correlated with the wavelengths, as was found to be the case by Brown and Scholz (1985). In other words, the small-wavelength roughness will usually be of small amplitude; which is to say that there will be no sharp dagger-like peaks in the aperture profile. They found that as long as the results are expressed in terms of $<h>$ and σ_h^2, the relationship between h_H, $<h>$, and σ_h was essentially unaffected. Hence, it seems that there is much evidence to support eq. (57) as an estimate of the hydraulic aperture in terms of only the mean and standard deviation of the aperture distribution. Of course, if the details of the aperture distribution are known, the geometric mean of h can also be used to estimate h_H, since (Piggott and Elsworth,

1993)

$$h_H^3 = k_{eff} \approx k_G = e^{<\ln k>} = e^{<\ln(h^3)>} = e^{3<\ln h>} = (e^{<\ln h>})^3 = h_G^3 . \qquad (58)$$

This latter estimate seems to be accurate to at least $O(\sigma_Y^6)$ for lognormal aperture distributions (Dagan, 1993), but it is not clear that eq. (58) is preferable to eq. (57) in the general case. For example, the numerical simulations of Piggott and Elsworth (1992) indicated that the geometric mean is a very poor predictor of the effective conductivity when the conductivity follows a bimodal distribution, particularly in two dimensions (see also Warren and Price, 1960, Fig. 7).

Effect of Contact Areas

As mentioned above, the areas where the rock faces are in contact with each other can be thought of as regions where the aperture is zero. However, most of the methods used to estimate or bound h_H will break down if the aperture distribution function ever takes on the value of zero. For example, the harmonic mean of k, which provides a lower bound to the effective conductivity, (see eq. (39b)), will degenerate to zero in these cases, as will the the geometric mean, since a finite probability of having $k = 0$ will cause $<\ln(k)> \rightarrow -\infty$. Note that a lognormal distribution of apertures does not allow the aperture to equal zero, since if $\ln(h)$ varies from $-\infty$ to $+\infty$ but vanishes as $\ln(h) \rightarrow \pm\infty$, h will take on only positive values. This suggests using methods such as those discussed above for the regions where the fracture is open, and treating the contact regions by separate methods. This approach has been taken by, for example, Walsh (1981) and Piggott and Elsworth (1992).

To isolate the effect of contact areas, we consider a fracture for which the aperture is uniform and equal to h_o, except for isolated contact regions where $h = 0$ (see Fig. 6). As usual, flow through this sort of geometry could, in principle, be analyzed

by solving the full Navier-Stokes equations. Since this approach is not feasible, we again reduce the governing equations to a more tractable form. Following the procedure by which the lubrication equation was derived for cases where the aperture was smoothly-varying, but nonzero, we find that we again require

$$Re^* \equiv \frac{\rho U h^2}{\mu \Lambda} \ll 1, \qquad \text{and} \qquad h/\Lambda \ll 1, \tag{59}$$

where now the characteristic lengthscale in the plane of the fracture, Λ, should be identified with, say, the dimensions in the (x,y) plane of the typical contact region (see Fig. 6). We again arrive at the lubrication equation (32b), except that since $h=0$ in those regions of the plane where the fracture faces are in contact, the equation has no meaning in those regions. Hence, we can only use this equation in the unobstructed regions, where $h(x,y)=h_o$, in which case eq. (32b) reduces to Laplace's equation:

$$\nabla^2 p(x,y) \equiv \frac{\partial^2 p}{\partial x^2} + \frac{\partial^2 p}{\partial y^2} = 0. \tag{60}$$

This mathematical model of flow between a pair of parallel plates that are obstructed by cylindrical posts is known as the Hele-Shaw model (Bear, 1972, pp. 687-692).

The boundaries of the contact regions must be treated as boundaries of the region in the (x,y) plane where this equation is to be solved. Consider one of these boundaries, which will be denoted by Γ_i. Since no fluid can enter the contact region, the component of the velocity vector normal to Γ_i must be zero. Eqs. (30) or (31) show that the velocity vector is parallel to the pressure gradient, so we see that

$$\frac{\partial p}{\partial n} \equiv (\nabla p)\cdot \mathbf{n} = 0, \tag{61}$$

where $\mathbf{n}$ is the outward unit normal vector to Γ_i, and n is the scalar coordinate in the direction of n. If we consider a rectangular region such as shown in Fig. 6, with uniform pressures on the $x=0$ and $x=L_x$ boundaries, no flow on the $y=0$ and $y=L_y$ boundaries, and no flow across the interior boundaries Γ_i, we have a well-posed boundary value problem for Laplace's equation, which will therefore have a unique solution (see Bers et al., 1964, pp. 152-154).

One problem that arises is that, in general, the solution to this problem will *not* satisfy the no-slip boundary conditions on the internal boundaries Γ_i. In physical terms, the Hele-Shaw solution does not account for viscous drag along the *sides* of the posts. The no-slip condition specifies that not only must the normal component of the velocity vanish, but so must the *tangential* component. However, if the components of the velocity vector are zero in two mutually orthogonal directions at each point on Γ_i, then the velocity components $\{u_x, u_y\}$ must both be zero. But the Hele-Shaw solution will generally yield a nonzero velocity u_t, where t is the local coordinate tangential to Γ_i. Hence, the Hele-Shaw solution will be in error in a certain region surrounding each contact area. In the original mathematical derivation of the the Hele-Shaw equations, Stokes (1905, p. 278) hypothesized that the region where the error is appreciable will be limited to a thin layer surrounding each Γ_i, the extent of which in the (x,y) plane will be of order h_o. This was verified by Thompson (1968), who developed a perturbation solution to the Stokes creeping flow equations, eq. (27), for flow between two parallel plates that are propped open by a single obstacle, the planform of which in the (x,y) plane is a circle of radius a. Thompson used the method of matched asymptotic expansions to piece together a solution valid near the obstacle, and another valid far from the obstacle, and found that the relative discrepancy between the Stokes and Hele-Shaw models was indeed on the order of h_o/a. In fact, he found that the relative error in the prediction of the effect that the obstacle has on reducing the flux, for a given far-field pressure gradient, was $1.26h_o/a$. However, this discrepancy is

already something of a higher-order effect, in the sense that the parallel plate conductance, $h_o^3/12$, is the zeroth-order result, and the first-order correction, which is captured by the Hele-Shaw model, is due to the fact that the fluid must follow a tortuous path around the obstacles. The additional factor of viscous drag on the sides of the post-like obstacles, which is not accounted for by the Hele-Shaw model, will generally be smaller still than the Hele-Shaw tortuosity correction, since h_o/a will typically be less than one. For example, the findings of Pyrak-Nolte et al. (1987) indicate that typical average apertures of fractures in crystalline rock are on the order of $10^{-4}-10^{-5}$ m, while asperity sizes (in the fracture plane) are on the order of $10^{-1}-10^{-3}$ m. Gale et al. (1990) measured apertures and asperity dimensions on a natural fracture in a granite from Stripa, Sweden, under a normal stress of 8 MPa, and found average values of $h \approx 0.1$ mm, $a \approx 1.0$ mm.

Kumar et al. (1991) used the Brinkman (1947) equation to further analyze the deviations from the Hele-Shaw model caused by finite values of h_o/a. Whereas the Hele-Shaw equation is derived by integrating the Stokes equations across the thickness of the fracture, the Brinkman equation can be "derived" by integrating the equations in the y-direction, which is the direction in the plane of the fracture, perpendicular to the direction of the mean flow. The obstacles are then not explicitly included in the geometry of the problem, but their effect on retarding the flow is represented by a distributed body force that is proportional to the velocity. This body force is found by solving the problem of flow past an array of infinitely long, parallel cylinders (Howells, 1974; Sangani and Yao, 1988). The results of the Brinkman analysis, along with the experimental data collected from various sources by Zimmerman and Kumar (1991), show that as long as $h_o/a < 1$, deviations from the Hele-Shaw conductivity will be less than 10%.

The problem of creeping flow through a smooth-walled fracture of aperture h_o, propped open by an array of circular cylinders of radii $a \gg h_o$, therefore reduces to the

problem of finding the effective conductance of a two-dimensional medium of conductance k_o, and which contains a dispersion of non-conductive, circular obstacles. This is a typical problem in effective medium theory, although it is of a different sort than that discussed above in relation to the lubrication model, in which the conductivity varied *smoothly* in space. A review of some of the various methods that have been proposed to attack this type of two-component effective medium problem is given by Hashin (1983). Fortunately, the predictions of the various methods do not diverge appreciably until the areal concentration of obstacles approaches about 0.30, which exceeds the amount of contact area that occurs in rock fractures, which is usually less than 0.25 (Tsang and Witherspoon, 1981; Pyrak-Nolte et al., 1987). Hence, any reasonable effective medium theory that has been proposed for two-component systems can be used for this problem.

Walsh (1981) used the effective medium theory that was originally proposed by Maxwell (1873, pp. 360-365), who estimated the effective conductivity of a three-dimensional medium containing a dispersion of non-conductive spheres. In the terminology of the present discussion, Maxwell's method consists of calculating the decrease in flow due to a single obstacle of known size and shape, averaging this effect over all shapes and orientations of the obstacles, and then equating the resulting decrease in flow to that which would be caused by a single *circular* "obstruction" which has some effective conductivity k_{eff}. The basic solution of the effect of a single circular obstruction on a uniform flow field can be found in Carslaw and Jaeger (1959, p. 426). Utilizing this solution, and the procedure outlined by Maxwell, Walsh (1981) found that the circular obstacles decrease the conductance below the cubic law value by a factor $(1-c)/(1+c)$, where c is the fraction of the (x,y) plane that is occupied by asperity obstructions. Hence the hydraulic aperture can be expressed as

$$h_H^3 = h_o^3 \frac{1-c}{1+c} \,. \tag{62}$$

Zimmerman et al. (1992) used boundary element calculations to verify the accuracy of this result to within about 2% for asperity concentrations up to 0.25 (see also Chen, 1990). If eq. (57) were applied to a fracture that has aperture h_o with probability $(1-c)$ and aperture zero with probability c, it would predict $h_H^3 = h_o^3(1-1.5c+...)$, which to first order in c is somewhat, although not substantially, different from eq. (62).

Since the factor involving the asperity concentration c reflects the tortuosity induced into the streamlines by the obstacles, this factor would be expected to depend on the planform of the asperity region. Zimmerman et al. (1992) extended Walsh's result to the case where the asperities were a randomly-distributed collection of ellipses, oriented randomly so that the overall conductivity was isotropic. Their analysis utilized the basic solution to two-dimensional flow around an elliptical obstacle that was presented by Obdam and Veling (1987). For ellipses of aspect ratio α, they found the hydraulic aperture to be given by

$$h_H^3 = h_o^3 \frac{1-\beta c}{1+\beta c}, \quad \text{where} \quad \beta = \frac{(1+\alpha)^2}{4\alpha}. \tag{63}$$

The factor β defined in eqn. (63) is always greater than unity, and monotonically increases as the ellipse becomes more elongated. Hence, elliptical obstacles obstruct the flow to a greater degree than do circular obstacles. This is consistent with the fact that Walsh's expression for circular obstacles coincides with the theoretical upper bound on k_{eff}/k_o that was derived using variational principles by Hashin and Shtrikman (1962) for a two-component medium, the components of which had conductivities k_o and 0. The factor β depends weakly on α as long as the obstacles are not very elongated. For example, an aspect ratio of 2 leads to $\beta = 1.125$, and $\alpha = 3$ yields $\beta = 1.33\overline{3}$. Although actual contact areas in fractures are not perfectly elliptical in

planform, Zimmerman et al. (1992) showed that eq. (63) can be applied to a smooth-walled fracture propped open by irregularly-shaped asperities, if the actual asperities are "replaced" by ellipses that have the same perimeter/area ratio.

Another method of accounting for the tortuosity caused by contact areas would be to use the effective medium theory of Kirkpatrick (1973). This model, originally developed to estimate the conductivity of random electrical networks, does not assume any particular shape for the asperity areas, but can be interpreted as corresponding to a checkerboard-like geometry in which each block is randomly assigned an aperture from the actual aperture distribution function. In the present context, this corresponds to each block having either aperture h_o with probability $(1-c)$, or aperture 0 with probability c. The finite-difference representation of conduction on such a checkerboard geometry would be a square lattice of conductors, in which case Kirkpatrick's theory predicts that

$$h_H^3 = h_o^3(1-2c) \; . \tag{64}$$

This model has many arguments in favor of its use. Firstly, it does not require any information concerning the geometrical shapes and distribution of the contact areas, other than the assumption that these areas are in some sense irregular, which is reasonable. At low concentrations, it asymptotically agrees with Walsh's result for circular asperities, since each give a tortuosity factor of $(1-2c)$, to first order in c. It also predicts a tortuosity factor that is always less than the Hashin-Shtrikman upper bound, which is $(1-c)/(1+c)$. Finally, it correctly predicts the existence of a *percolation* limit, which is a critical value of the contact area (in this case, 0.50) at which flow is completely obstructed. Although it seems reasonable that a sufficiently large amount of contact area will block off all flow paths, contact areas as large as 0.50 have not been reported very often in the literature, so for practical purposes this issue may be moot.

Nevertheless, the fact that eq. (64) incorporates the percolation phenomenon in some manner strengthens its utility as an estimate of the tortuosity.

Comparison of Models to Experimental Data

The question we now address is whether or not the various models and approximations presented and discussed above can be used to quantitatively relate the hydraulic conductance of a fracture to measured values of the aperture. We will not consider issues related to the process of making measurements of the aperture either in the field or in the laboratory, which are discussed by Gentier et al. (1989), Hakami and Barton (1990), and Johns et al. (1993), among others. We assume that data are available pertaining to the distribution function of the apertures, and also on the amount (and possibly the shapes) of the contact regions. The question we pose is how these data can be used to predict the conductivity, bearing in mind that in many cases, one might actually be more interested in the inverse problem of determining apertures and contact areas from conductivity data.

Although many measurements of fracture surface roughness have been reported in the literature, as well as many measurements of fracture conductivity, there are very few data sets in which both aperture data and hydraulic conductivity have been measured on the same fracture. One difficulty is that of relating the roughness measured for a single fracture surface to the aperture formed between two opposing surfaces when they are in contact (cf., Brown et al., 1986; Wang et al., 1988). Many of the measurements upon which certain widely-used roughness-conductivity correlations are based were actually made on artificially-roughened channels, the aperture profiles of which bore little resemblance to those of real fractures (Lomize, 1951; Louis, 1969). We will discuss only those available data sets in which measured fracture conductivities can be directly compared to aperture measurements made on the same fractures.

Comparisons between the various models and the measured values will be made on the basis of the cube of the hydraulic aperture, h_H^3, which is essentially equivalent to the transmissivity, aside from the factor of 12. The hydraulic apertures will be predicted using eight different schemes that are suggested by the previously-discussed analyses. These include using $\langle h \rangle^3$, $\langle h^3 \rangle$, h_G^3, and $\langle h \rangle^3[1-1.5\sigma_h^2/\langle h \rangle^2]$. In each case, the averages will be taken over those portions of the fracture that are not in contact and thereby closed to flow. If the fractional contact area c is known, predictions will also be made by correcting the above values by the tortuosity factor $(1-2c)$, as discussed above.

Gale et al. (1990) measured the apertures and conductivities of two fractures in a quartz monzonite granite from Stripa, Sweden, using a resin-impregnation technique that allowed aperture measurements to be made on the fracture under the same stress conditions as were used in the flow tests; further experimental details can be found in their report. Data from their two samples, which were taken from the same rock core, are shown in Table 1, along with the various predicted values of h_H^3. The values of $\langle h \rangle$ and σ_h were computed directly by Gale et al. (1990). We computed $\langle h^3 \rangle$ by assuming that the distribution was lognormal, which is shown by their Figs. 3.19 and 3.31 to be a reasonably accurate assumption, in which case eq. (55) can be used to show that $\langle h^3 \rangle = \langle h \rangle^9 / h_G^6$. The values used for h_G are arithmetic means of the h_G values measured on four profiles from each fracture. Since in each case all four profiles were statistically very similar, this method of averaging h_G should yield nearly the same result as would be found by averaging all the individual values of $\ln h$. Table 1 shows that use of the mean aperture $\langle h \rangle$ in the cubic law, even if corrected for the contact area, will greatly overestimate the actual conductivity. Use of $\langle h^3 \rangle$, as was suggested by Neuzil and Tracy (1981), will result in even greater error. The geometric mean h_G is somewhat more accurate, particularly if corrected for the effect of contact area. The most accurate predictions of h_H are those made by using the

two-term perturbation estimate, eq. (57), in conjunction with the tortuosity correction, $(1-2c)$. Note that for both fractures, a more accurate prediction could be made by assuming that the contact areas were non-circular, and using the tortuosity factor given by eq. (63). As it is not possible to objectively estimate the equivalent aspect ratio of the contact areas from the available data, we have used Kirkpatrick's "random lattice" tortuosity factor. Although Brown (1987) did not use precisely the same hydraulic aperture predictions as used in Table 1 to compare against his numerical solutions of the lubrication equations, it is worth noting that he also found that $<h>^3$ was a more accurate predictor of h_H^3 than was $<h^3>$, and that $<h>^3(1-c)/(1+c)$ was still more accurate.

Aperture and hydraulic conductivity measurements were made by Hakami (1989; see also Hakami and Barton, 1990) on epoxy replicas of fractures in five granite cores from Stripa. Sample A was a fine-grained granite, sample B was a leptite, and samples {S2,S3,S4} were quartz monzonites. Mean apertures, averaged over areas of about $1\,cm^2$, were found by injecting a known volume of dyed water into the fracture at various locations, and dividing the volume of the water drop by the observed area it occupied in the plane of the fracture. Although no contact area percentages were reported, the photographs shown of the water drops (Hakami, 1989, p. 46), as well as the aperture histograms at different stress levels (ibid., p. 67), seem to imply that contact area was minimal. We will therefore assume $c=0$ in our calculations. The assumption of minimal contact area is also consistent with the fact that the aperture measurements were made under very low values of normal stress (ibid., p. 66). Experimental values, and the various predictions of the hydraulic aperture, are shown in Table 2 for Hakami's five samples; sample A was measured under two different stresses. We used the values of $<h>$ and σ_h corresponding to the best log-normal fit to the aperture distributions; in most cases these values were well within 10% of the actual values, but for sample S3 this has the effect of ignoring a few anomalously high

apertures, which would alter σ_h, but would not be expected to affect h_H. Of the four methods of estimating h_H^3, eq. (57) is in general the most accurate, followed by h_G^3, $<h>^3$, and then $<h^3>$. In five of the six cases, both eq. (57) and the geometric mean yield conductivities that are within a factor of two of the measured value. In one case, A1, which was sample A tested under a nonzero normal stress, the measured conductance was extremely low, and was not accurately predicted by any of the methods. No explanation was given for the extremely low permeability measured in this test. Excluding this anomalous case, eq. (57) had an average error (in absolute value) of 21.5%, whereas the geometric mean had an average error of 42.1%. The fact that eq. (57) did not systematically overestimate the conductivity supports our assumption that the contact area correction factor is negligible for these cases.

For both sets of data discussed above, we have found that the expression

$$h_H^3 \approx <h>^3 \left[1 - \frac{3}{2}\frac{\sigma_h^2}{<h>^2}\right](1-2c) \tag{65}$$

usually provides a good estimate of the fracture conductivity. In fact, it was generally superior to the use of the cube of the geometric mean aperture, even after correction for the tortuosity due to contact area. This latter estimate is equivalent to that suggested by Piggott and Elsworth (1992), with $(1-2c)$ used as their tortuosity factor τ. (In contrast to the definition used in the petroleum literature, here the tortuosity factor is defined to be a multiplicative constant that is <1, rather than a factor that appears in the denominator and is >1.) Since there is much theoretical evidence in support of use of the geometric mean in the case of two-dimensional lognormal distributions, whereas the correction given by eq. (57) is only an $O(\sigma^2)$ perturbation approximation, these results call for some explanation. One point to bear in mind is that the actual distributions always deviate somewhat from being lognormal, and in such cases h_G should

only be a first-order estimate of h_H. Hence, h_G and eq. (57) are both first approximations to h_H, each in a different sense, for distributions that are slightly perturbed from lognormal. Another point is that some error is introduced when replacing the Navier-Stokes equations with the lubrication equation, eq. (32), due to finite values of $<h>/\lambda$, as was discussed previously. Eq. (35) implies that these errors tend to *reduce* the effective conductivity below the value predicted by the lubrication model. This may explain the fact that h_G overestimates h_H. If this explanation is correct, it may be fortuitous that eq. (57) just happens to "err" in the right direction.

Summary

We have discussed the problem of fluid flow through a rock fracture, treating it as a problem in fluid mechanics. First, the "cubic law" was derived as an exact solution to the Navier-Stokes equations for flow between smooth, parallel plates. For more realistic geometries, the Navier-Stokes equations cannot be solved in closed form, and they must be reduced to simpler equations. The various geometric and kinematic conditions that are necessary in order for the Navier-Stokes equations to be replaced by the lubrication or Hele-Shaw equations were then studied. A review was given of analytical and numerical studies of the lubrication equation for a rough-walled fracture. Several analytical and numerical studies lead to the conclusion that the hydraulic aperture can be predicted (see eqs. 37,57,58) from knowledge of the mean and the standard deviation of the aperture distribution. We showed that one can account for the tortuosity effect caused by regions where the rock walls are in contact with each other by a relatively simple correction factor, given by eq. (64), that depends only on the fractional amount of contact area. Finally, comparison was made between the various predictions of h_H, and the measured values, for eight data sets from two different research groups in which apertures and conductivities were available on the same fracture. The results showed that, in general, reasonably accurate predictions of

conductivity could be made by combining either the perturbation result, eq. (57), or the geometric mean, eq. (58), with the tortuosity factor given by eq. (64).

Acknowledgments

This work was carried out under U.S. Department of Energy Contract No. DE-AC03-76SF00098, for the Director, Office of Civilian Radioactive Waste Management, Office of Geologic Disposal, and was administered by the Nevada Operations Office, U. S. Department of Energy, in cooperation with the United States Geological Survey, Denver. The authors thank Akhil Datta Gupta and Curt Oldenburg of LBL, Lynn Gelhar of MIT, and Ron Linden of the DOE, for reviewing this report.

References

Aitchison, J. and Brown, J. A. C. (1957). *The Lognormal Distribution*, Cambridge University Press, New York.

Batchelor, G. K. (1967). *An Introduction to Fluid Dynamics*, Cambridge University Press, New York.

Bear, J. (1972). *Dynamics of Fluids in Porous Media*, Elsevier, New York.

Beran, M. J. (1968). *Statistical Continuum Theories*, Interscience, New York.

Bers, L., John, F., and Schechter, M. (1964). *Partial Differential Equations*, Wiley-Interscience, New York.

Brinkman, H. C. (1947). A calculation of the viscous force exerted by a flowing fluid on a dense swarm of particles, *Appl. Sci. Res.* A1, 27-34.

Brown, S. R. (1987). Fluid flow through rock joints: the effect of surface roughness, *J. Geophys. Res.* 92, 1337-1347.

Brown, S. R. (1989). Transport of fluid and electric current through a single fracture, *J. Geophys. Res.* 94(B7), 9429-9438.

Brown, S. R. and Scholz, C. H. (1985). Broad bandwidth study of the topography of natural rock surfaces, *J. Geophys. Res.* 90(B14), 12575-12582.

Brown, S. R., Kranz, R. L., and Bonner, B. P. (1986). Correlation between the surfaces of natural rock joints, *Geophys. Res. Letts.* 13, 1430-1433.

Carslaw, H. S. and Jaeger, J. C. (1959). *Conduction of Heat in Solids*, Oxford University Press, Oxford.

Chen, D. W. (1990). *Coupled stiffness-permeability analysis of a single rough-surfaced fracture by the three-dimensional boundary-element method*, Ph.D. dissertation, University of California, Berkeley.

Coulaud, O., Morel, P., and Caltagirone, J. P. (1991). Numerical modeling of non-linear effects in laminar flow through a porous medium, *J. Fluid Mech.* 190,

393-407.

Dagan, G. (1979). Models of groundwater flow in statistically homogeneous porous formations, *Water Resour. Res.* 15, 47-63.

Dagan, G. (1993). Higher-order correction of effective permeability of heterogeneous isotropic formations of lognormal conductivity distribution, *Transp. Porous Media* 12, 279-290.

de Marsily, G. (1986). *Quantitative Hydrogeology,* Academic Press, San Diego, Calif.

Elrod, H. G. (1979). A general theory for laminar lubrication with Reynolds roughness, *J. Lubr. Tech.* 101, 8-14.

Gale, J., MacLeod, R., and LeMessurier, P. (1990). Site characterization and validation - Measurement of flowrate, solute velocities and aperture variation in natural fractures as a function of normal and shear stress, stage 3, *Stripa Project Report 90-11*, Swedish Nuclear Fuel and Waste Management Company, Stockholm.

Geertsma, J. (1974). Estimating the coefficient of inertial resistance in fluid flow through porous media, *Soc. Petrol. Eng. J.* 14, 445-450.

Gentier, S., Billaux, D., and van Vliet, L. (1989). Laboratory testing of the voids of a fracture, *Rock Mech. Rock Eng.*, 22, 149-157.

Gomberg, J. (1991). U. S. Geological Survey Committee for the Advancement of Science in the Yucca Mountain Project Symposium on "Fractures, Hydrology, and Yucca Mountain": Abstracts and Summary, *U. S. Geological Survey Open-File Report 91-125.*

Gutjahr, A. L., Gelhar, L. W., Bakr, A. A., and MacMillan, J. R. (1978). Stochastic analysis of spatial variability in subsurface flows 2. Evaluation and application, *Water Resour. Res.* 14, 953-959.

Hakami, E. (1989). *Water Flow in Single Rock Joints*, Licentiate thesis, Lulea University of Technology, Lulea, Sweden.

Hakami, E. and Barton, N. (1990). Aperture measurements and flow experiments using transparent replicas of rock joints, in *Rock Joints: Proceedings of the International Symposium on Rock Joints*, N. Barton and O. Stephansson, eds., Balkema, Rotterdam, pp. 383-390.

Hasegawa, E. and Izuchi, H. (1983). On steady flow through a channel consisting of an uneven wall and a plane wall, Part 1, Case of no relative motion in two walls (sic), *Bull. Jap. Soc. Mech. Eng.* 26, 514-520.

Hashin, Z. (1983). Analysis of composite materials - A survey, *J. Appl. Mech.* 50, 481-505.

Hashin, Z. and Shtrikman, S. (1962). A variational approach to the theory of the effective magnetic permeability of multiphase materials, *J. Appl. Phys.* 33, 3125-3131.

Horne, R. N. and Rodriguez, F. (1983). Dispersion in tracer flow in fractured geothermal systems, *Geophys. Res. Letts.* 10, 289-292.

Howells, I. D. (1974). Drag due to the motion of a Newtonian fluid through a sparse random array of small fixed rigid objects, *J. Fluid Mech.* 64, 449-475.

Johns, R. A., Steude, J. S., Castanier, L. M., and Roberts, P. V. (1993). Nondestructive measurements of fracture aperture in crystalline rock cores using X ray computed tomography, *J. Geophys. Res.* 98, 1889-1900.

Jung, R. (1989). Hydraulic *in situ* investigations of an artificial fracture in the Falkenberg granite, *Int. J. Rock. Mech.* 26, 301-308.

Kirkpatrick, S. (1973). Percolation and conduction, *Rev. Mod. Phys.* 45, 574-588.

Kumar, S., Zimmerman, R. W., and Bodvarsson, G. S. (1991). Permeability of a fracture with cylindrical asperities, *Fluid Dyn. Res.* 7, 131-137.

Landau, L. D. and Lifshitz, E. M. (1960). *Electrodynamics of Continuous Media*, Pergamon Press, New York.

Langlois, W. E. (1964). *Slow Viscous Flow*, Macmillan, New York.

Lee, J. S. and Fung, Y.C. (1969). Stokes flow around a circular cylindrical post confined between two parallel plates, *J. Fluid Mech.* 37, 657-670.

Lomize, G. M. (1951). *Filtratsiia v Treshehinovatykh Porod (Water Flow in Jointed Rock)*, Gosenergoizdat, Moscow.

Louis, C. (1969). *A Study of Groundwater Flow in Jointed Rock and its Influence on the Stability of Rock Masses*, Ph.D. dissertation, Imperial College, London.

Maxwell, J. C. (1873). *A Treatise on Electricity and Magnetism*, Clarendon Press, Oxford.

Murphy, J. R. and Thomson, N. R. (1993). Two-phase flow in a variable-aperture fracture, *Water Resour. Res.* 29, 3453-3476.

Neuzil, C. E. and Tracy, J. V. (1981). Flow through fractures, *Water Resour. Res.* 17, 191-199.

Obdam, A. N. M. and Veling, E. J. M. (1987). Elliptical inhomogeneities in groundwater flow - an analytical description, *J. Hydrol.* 95, 87-96.

Patir, N. and Cheng, H. S. (1978). An average flow model for determining effects of three-dimensional roughness on partial hydrodynamic lubrication, *J. Lubr. Technol.* 100, 12-17.

Phillips, O. M. (1991). *Flow and Reaction in Permeable Rocks,* Cambridge University Press, New York.

Piggott, A. R. and Elsworth, D. (1992). Analytical models for flow through obstructed domains, *J. Geophys. Res.* 97, 2085-2093.

Piggott, A. R. and Elsworth, D. (1993). Laboratory assessment of the equivalent apertures of a rock fracture, *Geophys. Res. Letts.* 20, 1387-1390.

Pozrikidis, C. (1987). Creeping flow in two-dimensional channels, *J. Fluid Mech.* 180, 495-514.

Pozrikidis, C. (1992). *Boundary integral and singularity methods for linearized viscous flow,* Cambridge University Press, New York.

Pruess, K. and Tsang, Y. W. (1990). On two-phase relative permeability and capillary pressure or rough-walled rock fractures, *Water Resour. Res.* 26, 1915-1926.

Pyrak-Nolte, L. J., Myer, L. R., Cook, N. G. W., and Witherspoon, P. A. (1987). Hydraulic and mechanical properties of natural fractures in low permeability rock, in *Proceedings of the 6th International Congress of Rock Mechanics*, G. Herget and S. Vongpaisal, eds., Balkema, Rotterdam, pp. 225-231.

Reynolds, O. (1886). On the theory of lubrication, *Phil. Trans. Roy. Soc. London* 177, 157-134.

Sangani, A. S. and Yao, C. (1988). Transport processes in random arrays of cylinders. II. Viscous flow, *Phys. Fluids* 31, 2435-2444.

Schlichting, H. (1968). *Boundary-Layer Theory, 6th ed.,* McGraw-Hill, New York.

Sherman, F. (1990). *Viscous Flow*, McGraw-Hill, New York.

Silliman, S. E. (1989). An interpretation of the difference between aperture estimates derived from hydraulic and tracer tests in a single fracture, *Water Resour. Res.* 25, 2275-2283.

Sokolnikoff, I. S. (1956). *Mathematical Theory of Elasticity, 2nd ed.*, McGraw-Hill, New York, 1956.

Stokes, G. G. (1905). *Mathematical and Physical Papers*, Cambridge University Press, Cambridge.

Thompson, B. W. (1968). Secondary flow in a Hele-Shaw cell, *J. Fluid Mech.*, 31(2), 379-395.

Tsang, Y. W. and Witherspoon, P. A. (1981). Hydromechanical behavior of a deformable rock fracture subject to normal stress, *J. Geophys. Res.* B86, 9287-9298.

Tsay, R.-Y. and Weinbaum, S. (1991). Viscous flow in a channel with periodic cross-bridging fibers: exact solutions and Brinkman approximation, *J. Fluid Mech.* 226, 125-148.

Walsh, J. B. (1981). The effect of pore pressure and confining pressure on fracture permeability, *Int. J. Rock Mech.* 18, 429-435.

Wang, J. S. Y., Narasimhan, T. N., and Scholz, C. H. (1988). Aperture correlation of a fractal fracture, *J. Geophys. Res.* 93(B3), 2216-2224.

Warren, J. E. and Price, H. S. (1960). Flow in heterogeneous porous media, *Soc. Petrol. Eng. J.* 1, 153-169.

Witherspoon, P. A., Wang, J. S. Y., Iwai, K., and Gale, J. E. (1980). Validity of cubic law for fluid flow in a deformable rock fracture, *Water Resour. Res.* 16, 1016-1024.

Wright, D. E. (1968). Nonlinear flow through granular media, *Proc. Amer. Soc. Civ. Eng. Hydr. Div.* 94(HY4), 851-872.

Zimmerman, R. W. and Kumar, S. (1991). A fluid-mechanical model for blood flow in lung alveoli, in *Advances in Biological Heat and Mass Transfer*, ASME Heat Transfer Division Vol. 189, J. J. McGrath, ed., American Society of Mechanical Engineers, New York, pp. 51-56.

Zimmerman, R. W., Kumar, S., and Bodvarsson, G. S. (1991). Lubrication theory analysis of the permeability of rough-walled fractures, *Int. J. Rock Mech.* 28, 325-331.

Zimmerman, R. W., Chen, D. W., and Cook, N. G. W. (1992). The effect of contact area on the permeability of fractures, *J. Hydrol.*, 139, 79-96.

Nomenclature

Roman letters

a radius of asperity in fracture plane

c areal concentration of asperities

$\mathbf{F}$ body force vector, eq. (1)

$\mathbf{g}$ gravitational acceleration vector

g magnitude of $\mathbf{g}$

h aperture of fracture

$h_{1,2}$ half apertures, Fig. 2

h_H hydraulic aperture, eq. (18)

h_o nominal aperture of rough fracture

$<h>$ mean value of aperture

k local conductivity in lubrication model, $=h^3/12$

k_G geometric mean of conductivity

k_{eff} effective conductivity

L length of fracture in direction of mean flow

L_x length of fracture in direction of mean flow

L_y length of fracture normal to direction of mean flow

m dimension, = 2 for fracture flow; eq. (47)

n direction in fracture plane normal to the asperity boundary

p pressure

p_i pressure at inlet to fracture

p_o pressure at outlet to fracture

$\hat{p}$ reduced pressure, $=p+\rho gz$; eq. (3)

Q volumetric flowrate

Re Reynolds number; eq. (19)

Re^* reduced Reynolds number; eq. (25)

t time

T transmissivity of fracture; eq. (16)

$\mathbf{u}$ velocity vector

u_i velocity component in direction i

U order of magnitude of velocity

w width of fracture, normal to mean flow direction, in fracture plane

x direction of mean flow

y direction normal to mean flow, in fracture plane

Y $\ln(k)$, where k is the local fracture conductivity

z vertical direction

z direction normal to the fracture plane

Greek letters

α aspect ratio of elliptical contact region

β shape factor for effective conductivity; eq. (63)

Γ boundary of asperity (in fracture plane)

δ amplitude of sinusoidal aperture perturbation

ε relative roughness parameter, $=\langle h \rangle/\lambda$

Λ characteristic length in plane of fracture

μ viscosity of fluid

ρ density of fluid

σ_d standard deviation of aperture roughness function; eq. (38)

σ_h standard deviation of aperture distribution

σ_k standard deviation of conductivity

σ_Y standard deviation of log conductivity

∇ gradient operator

Table 1. Hydraulic transmissivities of fractures in quartz monzonite granite from Stripa, Sweden. Aperture data and measured conductivities are from Gale et al. (1990). Predictions of hydraulic apertures are made using methods described in the text. Transmissivity per unit width is equal to $h_H^3/12$.

Sample	S2	S3
$\langle h \rangle$	180 μm	223 μm
σ_h	106 μm	162 μm
c	.146	.349
$\langle h^3 \rangle$	7.54×10^{-12} m^3	51.8×10^{-12} m^3
$\langle h^3 \rangle(1-2c)$	5.34×10^{-12} m^3	15.6×10^{-12} m^3
$\langle h \rangle^3$	5.83×10^{-12} m^3	11.1×10^{-12} m^3
$\langle h \rangle^3(1-2c)$	4.13×10^{-12} m^3	3.35×10^{-12} m^3
h_G^3	5.13×10^{-12} m^3	5.13×10^{-12} m^3
$h_G^3(1-2c)$	3.63×10^{-12} m^3	1.55×10^{-12} m^3
$\langle h \rangle^3[1-1.5\sigma_h^2/\langle h \rangle^2]$	2.80×10^{-12} m^3	2.31×10^{-12} m^3
$\langle h \rangle^3[1-1.5\sigma_h^2/\langle h \rangle^2](1-2c)$	1.98×10^{-12} m^3	0.70×10^{-12} m^3
h_H^3 (measured)	1.12×10^{-12} m^3	0.34×10^{-12} m^3

Table 2. Hydraulic transmissivities of fractures in granite cores from Stripa, Sweden. Aperture data and measured conductivities are from Hakami (1989). Predictions of hydraulic apertures are made using methods described in the text. Transmissivity per unit width is equal to $h_H^3/12$.

	B	S2	S3	S4	A1	A2
$\langle h \rangle$	309	464	393	261	83	161
σ_h	193	273	295	98	34	72
$\langle h^3 \rangle$	79.24	243.71	231.98	26.46	0.912	7.209
$\langle h \rangle^3$	29.50	99.90	60.70	17.80	0.572	4.173
h_G^3	18.00	63.96	31.05	14.60	0.453	3.175
$\langle h \rangle^3[1-1.5\sigma_h^2/\langle h \rangle^2]$	12.24	48.03	9.40	14.04	0.428	2.921
h_H^3 (measured)	13.14	78.40	14.53	13.31	$<10^{-4}$	2.406

$\langle h \rangle$ and σ_h are given in units of μm; other values are in units of 10^{-12} m^3.

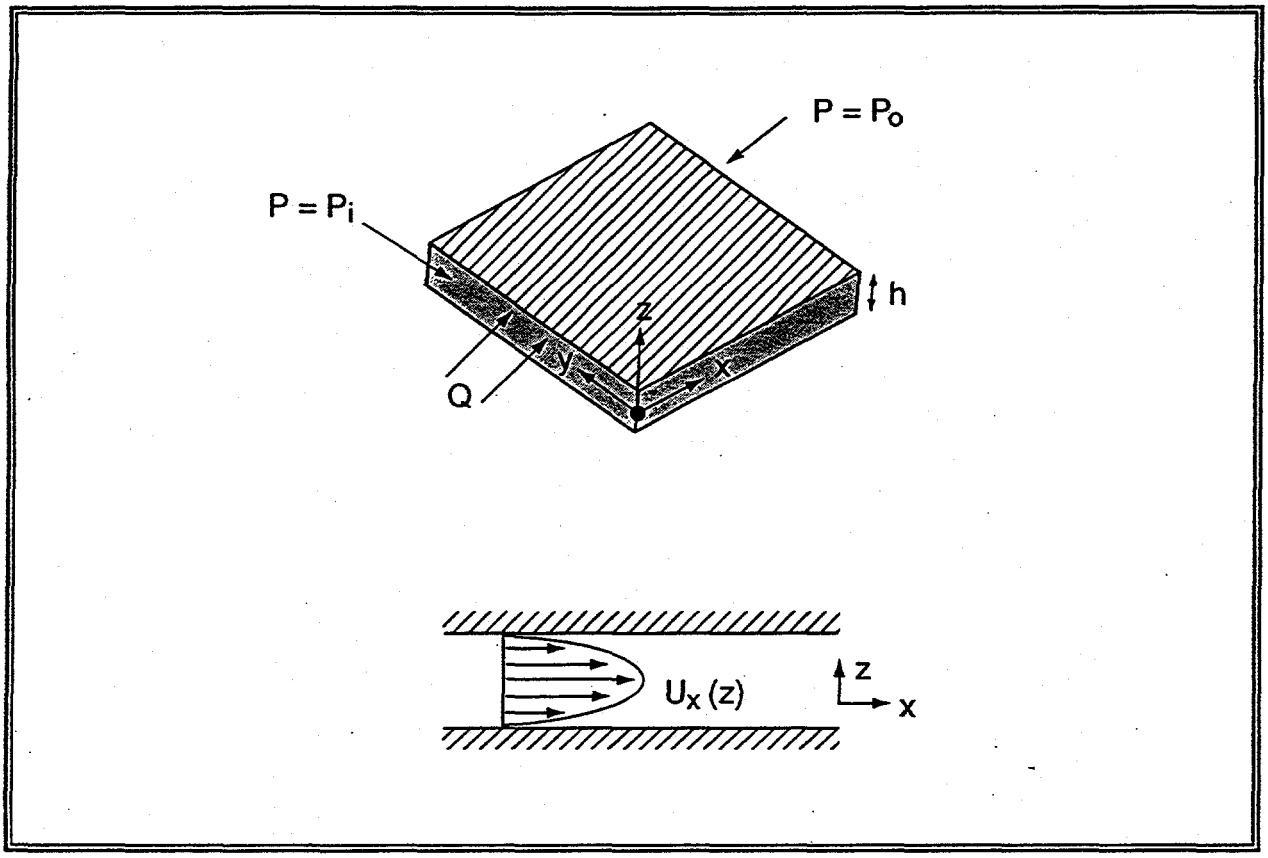

Fig. 1. Parallel-plate fracture of aperture h, with uniform pressures p_i and p_o imposed on two opposing faces. The resulting parabolic velocity distribution given by eq. (10) is shown in the lower cartoon.

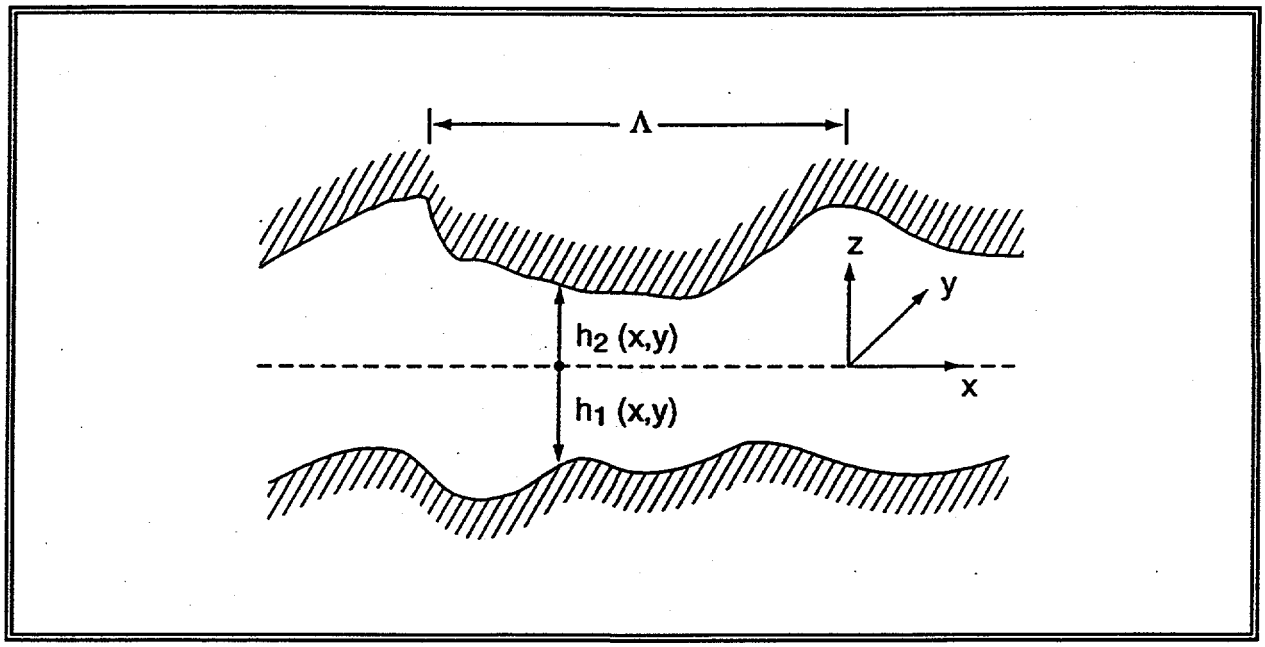

Fig. 2. Side view of a cross-section of a rough-walled rock fracture containing no contact areas. The two half-apertures are h_1 and h_2, both defined as positive. The characteristic length over which the aperture varies appreciably is denoted by Λ.

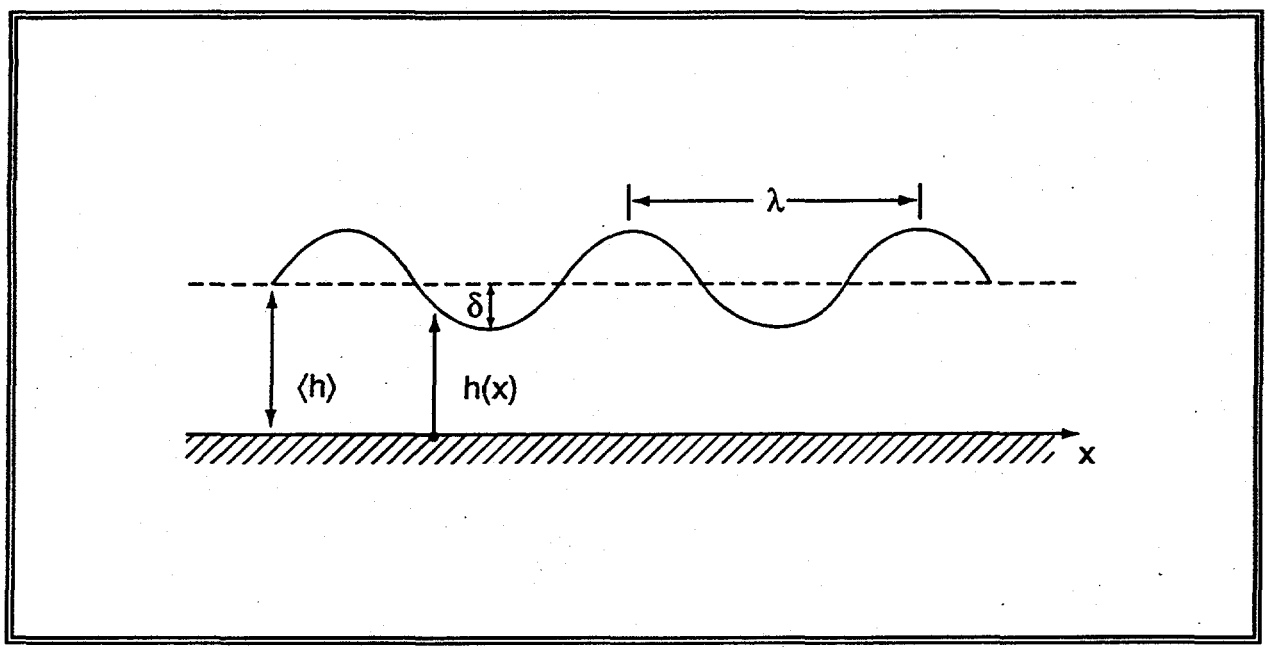

Fig. 3. Side view of a fracture channel consisting of one smooth wall and one sinusoidal wall, with the aperture given by eq. (34). The mean aperture is $\langle h \rangle$, the spatial wavelength is λ, and the amplitude of the aperture roughness is δ.

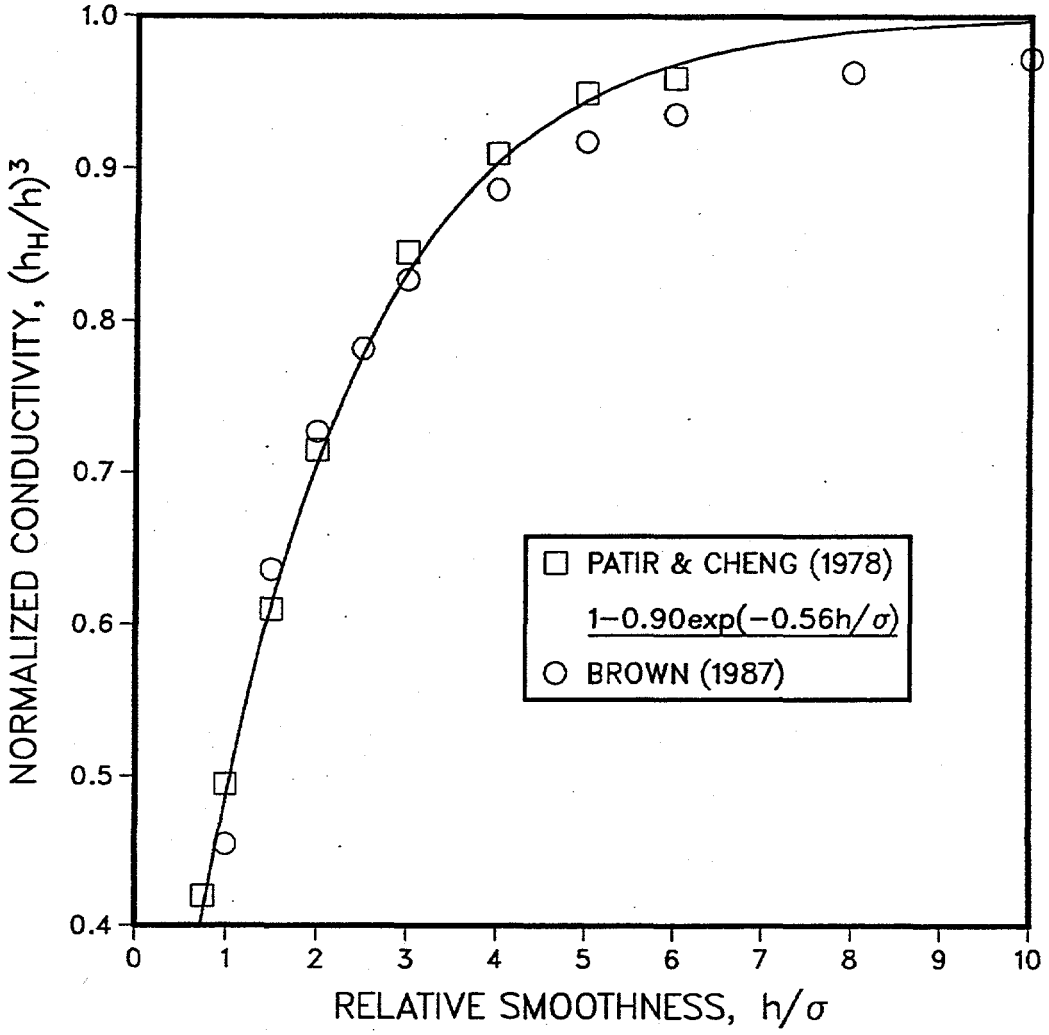

Fig. 4. Results found numerically by Patir and Cheng (1978) and Brown (1987) for the hydraulic aperture as a function of the relative roughness. The slightly different definitions used for h and σ are discussed in the text. Also plotted is eq. (37), which was fitted by Patir and Cheng to their numerical values.

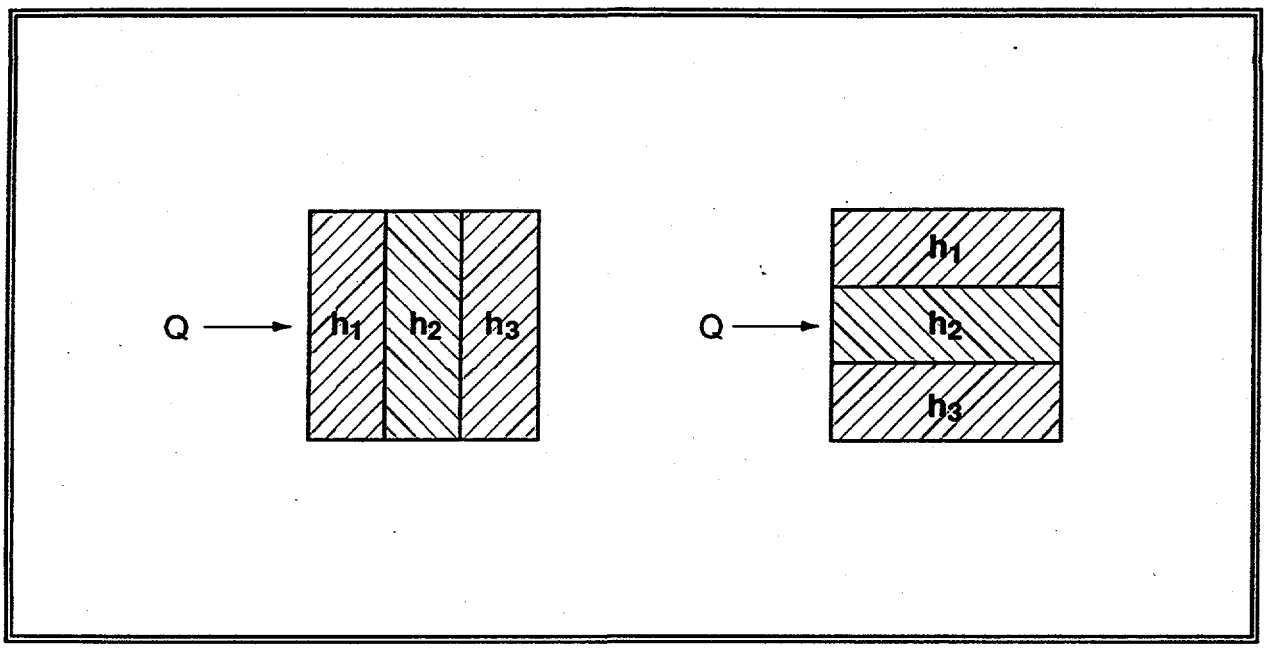

Fig. 5. Fracture in which the aperture varies either only in the direction of flow (top), or only in the direction transverse to the flow (bottom). First case leads to $h_H^3 = \langle h^{-3} \rangle^{-1}$, which is a lower bound on the actual isotropic conductivity. Second case leads to $h_H^3 = \langle h^3 \rangle$, which is an upper bound on the actual isotropic conductivity.

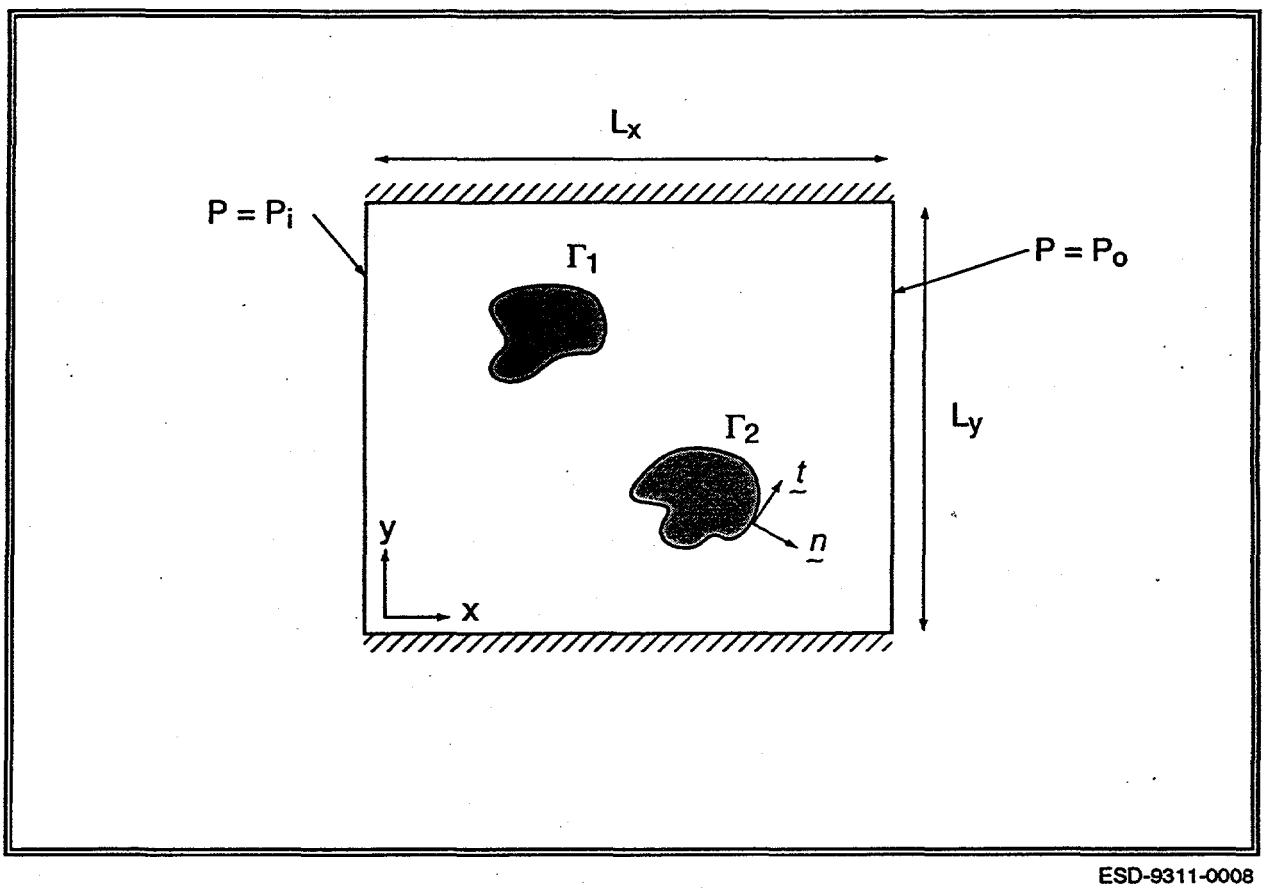

Fig. 6. Schematic diagram of computational problem for the Hele-Shaw model, with impermeable boundaries at $y=0$ and $y=L_y$, constant pressure boundaries at $x=0$ and $x=L_x$, and two internal impermeable boundaries that represent the asperity regions.